ELSEVIER

Contents lists available at ScienceDirect

Journal of Computational and Applied Mathematics

journal homepage: www.elsevier.com/locate/cam



An L^p- primal-dual weak Galerkin method for div-curl systems



Waixiang Cao a,1, Chunmei Wang b,*,2, Junping Wang c,3

- ^a School of Mathematical Science, Beijing Normal University, Beijing, 100875, China
- ^b Department of Mathematics, University of Florida, Gainesville, FL 32611, USA
- ^c Division of Mathematical Sciences, National Science Foundation, Alexandria, VA 22314, USA

ARTICLE INFO

Article history: Received 2 August 2022

2020 Mathematics Subject Classification: primary 65N30 35Q60 65N12 secondary 35F45 35O61

Keywords: Finite element methods Weak Galerkin methods Primal-dual weak Galerkin Div-curl system

ABSTRACT

This paper presents a new L^p -primal–dual weak Galerkin (PDWG) finite element method for the div–curl system with the normal boundary condition for p>1. Two crucial features for the proposed L^p -PDWG finite element scheme are as follows: (1) it offers an accurate and reliable numerical solution to the div–curl system under the low $W^{\alpha,p}$ -regularity ($\alpha>0$) assumption for the exact solution; (2) it offers an effective approximation of the normal harmonic vector fields on domains with complex topology. An optimal order error estimate is established in the L^q -norm for the primal variable where $\frac{1}{p}+\frac{1}{q}=1$. A series of numerical experiments are presented to demonstrate the performance of the proposed L^p -PDWG algorithm.

© 2022 Elsevier B.V. All rights reserved.

1. Introduction

In this paper we shall develop a new L^p -primal-dual weak Galerkin (PDWG) methods for the div-curl system with the normal boundary condition. To this end, we consider the model problem: Find a vector field u = u(x) such that

$$\nabla \cdot (\varepsilon \mathbf{u}) = f, \quad \text{in } \Omega, \tag{1.1a}$$

$$\nabla \times \mathbf{u} = \mathbf{g}, \quad \text{in } \Omega,$$
 (1.1b)

$$\varepsilon \mathbf{u} \cdot \mathbf{n} = \phi_1, \quad \text{on } \Gamma,$$

where $\Omega \subset \mathbb{R}^3$ is an open, bounded and connected polyhedral domain, and $\Gamma = \partial \Omega$ is the boundary of Ω . Assume that Γ is the union of a finite number of disjoint surfaces $\Gamma = \bigcup_{i=0}^L \Gamma_i$ with Γ_0 being the exterior boundary of Ω and Γ_i ($i=1,\ldots,L$) being the other connected components with finite surface areas. Note that L is equal to the number of holes in the domain Ω geometrically which is known as the second Betti number of Ω or the dimension of the second de

E-mail addresses: caowx@bnu.edu.cn (W. Cao), chunmei.wang@ufl.edu (C. Wang), jwang@nsf.gov (J. Wang).

- ¹ The research of Waixiang Cao was partially supported by National Science Foundation of China grants No. 11871106 and 12271049.
- ² The research of Chunmei Wang was partially supported by National Science Foundation Grants DMS-2136380 and DMS-2206332.
- ³ The research of Junping Wang was supported by the NSF IR/D program, while working at National Science Foundation. However, any opinion, finding, and conclusions or recommendations expressed in this material are those of the author and do not necessarily reflect the views of the National Science Foundation.

^{*} Corresponding author.

Rham cohomology group of Ω . Assume the coefficient matrix $\varepsilon = \{\varepsilon_{ij}(\mathbf{x})\}_{3\times 3}$ is symmetric and uniformly positive definite in Ω with ε_{ij} (i,j=1,2,3) being in $L^{\infty}(\Omega)$.

The solution uniqueness for the div–curl system (1.1a)–(1.1c) depends on the topology of the domain Ω . It is well-known that the solution uniqueness holds true for simply connected Ω , while the solution is unique up to a normal ε -harmonic function in $\mathbb{W}_0^{\varepsilon n,p}(\Omega)$ defined in (2.1) for the case that the domain Ω is not simply connected. The dimension of $\mathbb{W}_0^{\varepsilon n,p}(\Omega)$ is the first Betti number of Ω which is the rank of the first homology group of Ω .

The div–curl system (1.1a)–(1.1b) arises in many applications in science and engineering such as electromagnetic fields and fluid mechanics. Computational electro-magnetics plays an important role in many areas such as radar, satellite, antenna design, waveguides, optical fibers, medical imaging and design of invisible cloaking devices [1]. In linear magnetic fields, the function $f(\mathbf{x})$ vanishes, \mathbf{u} represents the magnetic field intensity and $\varepsilon(\mathbf{x})$ is the inverse of the magnetic permeability tensor. In fluid mechanics fields, the coefficient matrix $\varepsilon(\mathbf{x})$ is diagonal with diagonal entries being the local mass density. In electrostatics fields, $\varepsilon(\mathbf{x})$ is the permittivity matrix.

There have been several numerical methods proposed and analyzed for the div-curl system (1.1a)-(1.1b). A covolume method was developed by the employment of the Voronoi-Delaunay mesh pairs in three dimensional space [2], [3] developed a least-squares finite element method for two types of boundary value problems. The least-squares method was proposed in [4] for the div-curl problem based on discontinuous elements on nonconvex polyhedral domains, In [5], a classical numerical method was introduced for solving the magnetostatic problem by employing a scalar or vector potential. The control volume method [6] was proposed directly for planar div-curl problems. [7] proposed a discrete duality finite volume method for div-curl problems on almost arbitrary polygonal meshes. A mixed finite element method was introduced in [8] for three dimensional axisymmetric div-curl systems through a dimension reduction technique based on the cylindrical coordinates in simply connected and axisymmetric domains. The mimetic finite difference scheme [9,10] was introduced for the magneto-static problems on general polyhedral partitions. The numerical algorithm was designed to construct a finite element basis for the first de Rham cohomology group of the computational domain, which was further used for a numerical approximation of the magnetostatic problem. [11] proposed a weak Galerkin finite element method for the div-curl system with either normal or tangential boundary conditions. Another weak Galerkin scheme was introduced in [12] by using a least-squares approach for the div-curl problem. [13,14] developed primal-dual weak Galerkin finite element methods for the div-curl system with tangential boundary condition and normal boundary condition respectively and proved that the schemes work well for the exact solution with low-regularity assumptions. The primal-dual weak Galerkin finite element methods have been developed for many challenging PDEs (see an incomplete list [11.15-22])

There are two main challenges in the approximation of the div–curl system (1.1a)–(1.1c): (1) the low-regularity of the exact solution \boldsymbol{u} limiting the stability and accuracy of the numerical solutions, and (2) the non-uniqueness of the solution \boldsymbol{u} on domains with complex topology. The later one can be relaxed to certain extent by seeking a particular solution orthogonal to the space of normal ε -harmonic vector space $\mathbb{W}_0^{\varepsilon n,p}(\Omega)$, but with an immediate obstacle lying in the determination of the space $\mathbb{W}_0^{\varepsilon n,p}(\Omega)$ or an effective approximation of this space. To address these challenges, we shall devise a new L^p primal–dual weak Galerkin (PDWG) scheme for (1.1a)–(1.1c) by following the framework developed in [14]. It should be noted that the L^p -PDWG framework was originated in [23] for convection–diffusion equations. Our L^p -PDWG numerical method for (1.1a)–(1.1c) has two prominent features over the existing numerical methods: (1) it offers an effective approximation for the normal ε -harmonic vector space $\mathbb{W}_0^{\varepsilon n,p}(\Omega)$ regardless of the topology of the domain Ω ; and (2) it provides an accurate and reliable numerical solution for the div–curl system (1.1a)–(1.1c) with low $W^{\alpha,p}$ -regularity ($\alpha > 0$) assumption for the exact solution \boldsymbol{u} .

The paper is organized as follows. In Section 2, we introduce the notation and derive the weak formulation for the div–curl system (1.1a)–(1.1c). In Section 3 a L^p -PDWG algorithm for both the div–curl problem and the discrete normal ε -harmonic vector fields is proposed. The solution existence and uniqueness for the L^p -PDWG scheme is discussed in Section 4. The convergence theory for the L^p -PDWG approximation is established in Section 5. Finally, several test examples are demonstrated to illustrate the performance of the L^p -PDWG algorithm in Section 6.

2. Weak formulations

2.1. Notations

We follow the usual notations for Sobolev spaces and norms [24,25]. Let $D \subset \mathbb{R}^3$ be an open bounded domain with Lipschitz continuous boundary. Denote by $W^{div_\varepsilon,p}(D)$ the closed subspace of $[L^p(D)]^3$ such that $\nabla \cdot (\varepsilon v) \in L^p(D)$. Denote $W^{div_\varepsilon,p}(D)$ by $W^{div_\varepsilon,p}(D)$ when $\varepsilon = I$. Analogously, we use $W^{curl,p}(D)$ to denote the closed subspace of $[L^p(D)]^3$ so that $\nabla \times v \in [L^p(D)]^3$. Denote by $W^{curl,p}_0(D)$ the closed subspace with vanishing tangential boundary values, i.e.,

$$W_0^{\operatorname{curl},p}(D) := \{ \boldsymbol{v} \in W^{\operatorname{curl},p}(D), \ \boldsymbol{v} \times \boldsymbol{n} = 0 \text{ on } \partial D \}.$$

Denote by $\langle \cdot, \cdot \rangle_{\Gamma_i}$ the inner product in $L^2(\Gamma_i)$. We introduce the following Sobolev space

$$\mathbb{W}_{\varepsilon}(\Omega) = \{ \boldsymbol{v} \in W_0^{\operatorname{curl},p}(\Omega) \cap W^{\operatorname{div}_{\varepsilon},p}(\Omega), \ \nabla \cdot (\varepsilon \boldsymbol{v}) = 0, \ \langle \varepsilon \boldsymbol{v} \cdot \boldsymbol{n}_i, \ 1 \rangle_{\Gamma_i} = 0, \ i = 1, \ldots, L \}.$$

A vector field $\mathbf{v} \in [L^p(\Omega)]^3$ is defined to be ε -harmonic in Ω if it is ε -solenoidal and irrotational in Ω . Denoted by $\mathbb{W}_{0}^{\varepsilon n,p}(\Omega)$ the space of normal ε -harmonic vector fields that consists of all ε -harmonic vector fields satisfying vanishing normal boundary condition, i.e.,

$$\mathbb{W}_{0}^{\varepsilon n,p}(\Omega) = \{ \boldsymbol{v} \in [L^{p}(\Omega)]^{3} : \ \nabla \times \boldsymbol{v} = 0, \ \nabla \cdot (\varepsilon \boldsymbol{v}) = 0, \ \varepsilon \boldsymbol{v} \cdot \boldsymbol{n} = 0 \text{ on } \Gamma \}.$$
(2.1)

Denote $\mathbb{W}_{0}^{\varepsilon n,p}(\Omega)$ by $\mathbb{W}_{0}^{n,p}(\Omega)$ for $\varepsilon=I$. Similarly, denoted by $\mathbb{W}_{0}^{\varepsilon \tau,p}(\Omega)$ the space of tangential ε -harmonic vector fields that consists of all ε -harmonic vector fields satisfying vanishing tangential boundary condition, i.e.,

$$\mathbb{W}_0^{\varepsilon\tau,p}(\Omega) = \{ \boldsymbol{v} \in [L^p(\Omega)]^3 : \ \nabla \times \boldsymbol{v} = 0, \ \nabla \cdot (\varepsilon \boldsymbol{v}) = 0, \ \boldsymbol{v} \times \boldsymbol{n} = 0 \text{ on } \Gamma \}.$$

2.2. A weak formulation

Testing (1.1a) by any $\varphi \in W^{1,p}(\Omega)$ and using the normal boundary condition (1.1c) yields

$$(\mathbf{u}, \varepsilon \nabla \varphi) = \langle \phi_1, \varphi \rangle - (f, \varphi), \quad \forall \varphi \in W^{1,p}(\Omega).$$
 (2.2)

Testing (1.1b) by any $\mathbf{w} \in W_0^{curl,p}(\Omega)$ gives

$$(\boldsymbol{u}, \nabla \times \boldsymbol{w}) = (\boldsymbol{g}, \boldsymbol{w}), \quad \forall \boldsymbol{w} \in W_0^{\text{curl}, p}(\Omega).$$
 (2.3)

Combining with Eqs. (2.2) and (2.3), we obtain a weak solution $\boldsymbol{u} \in [L^q(\Omega)]^3$ ($\frac{1}{p} + \frac{1}{q} = 1$) of the div-curl system with normal boundary condition (1.1a)-(1.1c) satisfying

$$(\mathbf{u}, \varepsilon \nabla \varphi + \nabla \times \mathbf{\psi}) = (\mathbf{g}, \mathbf{\psi}) - (f, \varphi) + \langle \phi_1, \varphi \rangle, \tag{2.4}$$

for all $\varphi \in W^{1,p}(\Omega)$ and $\psi \in W_0^{curl,p}(\Omega)$. As discussed in [14], the solution to the variational problem (2.4) is non-unique in general. The homogeneous version of (2.4) is to seek a $\mathbf{u} \in [L^q(\Omega)]^3(\frac{1}{p}+\frac{1}{q}=1)$ satisfying

$$(\boldsymbol{u}, \varepsilon \nabla \varphi + \nabla \times \boldsymbol{\psi}) = 0 \qquad \forall \varphi \in W^{1,p}(\Omega), \ \forall \boldsymbol{\psi} \in W_0^{curl,p}(\Omega).$$
 (2.5)

Note that the solution could be any ε -harmonic function in $\mathbb{W}_0^{\varepsilon n,p}(\Omega)$ which is non-unique provided that the ε -harmonic space $\mathbb{W}_0^{\varepsilon n,p}(\Omega)$ has a positive dimension. The solution to the div–curl system (1.1a)–(1.1c) is unique provided that the solution is ε -weighted L^2 orthogonal to $\mathbb{W}_0^{\varepsilon n,p}(\Omega)$.

2.3. An extended weak formulation

In this subsection, we slightly modify the weak formulation (2.5) to ensure that the solution to the homogeneous version of (2.4) is unique.

We first denote by $W_{0c}^{1,p}(\Omega)$ the subspace of $W^{1,p}(\Omega)$ with vanishing value on Γ_0 and constant values on other connected components of the boundary; i.e.,

$$W_{0c}^{1,p}(\Omega) = \{ \phi \in W^{1,p}(\Omega) : \ \phi|_{\Gamma_0} = 0, \ \phi|_{\Gamma_i} = \alpha_i, \ i = 1, \dots, L \}.$$

Define the following bilinear form:

$$B(\mathbf{u}, \mathbf{s}; \varphi, \psi) := (\mathbf{u}, \varepsilon \nabla \varphi + \nabla \times \psi) + (\psi, \varepsilon \nabla \mathbf{s}). \tag{2.6}$$

Now the extended weak formulation for the div–curl system (1.1a)–(1.1c) seeks $(\boldsymbol{u},s) \in [L^q(\Omega)]^3 \times W^{1,p}_{0c}(\Omega)$ satisfying

$$B(\boldsymbol{u}, s; \varphi, \boldsymbol{\psi}) = F(\varphi, \boldsymbol{\psi}), \qquad \forall \varphi \in W^{1,p}(\Omega), \forall \boldsymbol{\psi} \in W_0^{\operatorname{curl},p}(\Omega), \tag{2.7}$$

where

$$F(\varphi, \psi) = (g, \psi) - (f, \varphi) + \langle \phi_1, \varphi \rangle. \tag{2.8}$$

The homogeneous dual problem of (2.7) seeks $(\lambda, \mathbf{q}) \in W^{1,p}(\Omega)/\mathbb{R} \times W_0^{curl,p}(\Omega)$ such that

$$B(\boldsymbol{v}, r; \lambda, \boldsymbol{q}) = 0, \qquad \forall \boldsymbol{v} \in [L^{q}(\Omega)]^{3}, \ \forall r \in W_{0c}^{1,p}(\Omega). \tag{2.9}$$

It has been proved in [14] that the solution to the homogeneous dual problem (2.9) is unique.

3. L^p -PDWG scheme

To design a L^p -PDWG scheme for the div-curl system (1.1a)-(1.1c), we first briefly review the definitions of discrete weak gradient and discrete weak curl [14] and then introduce some finite element spaces, which shall be used in our later algorithm.

Denote by \mathcal{T}_h a finite element partition of the domain Ω that consists of shape-regular polyhedra [26]. Denote by \mathcal{E}_h and $\mathcal{E}_h^0 = \mathcal{E}_h \setminus \partial \Omega$ the set of all faces and the set of all interior faces in \mathcal{T}_h respectively. Let h_T be the diameter of the element $T \in \mathcal{T}_h$ and $h = \max_{T \in \mathcal{T}_h} h_T$ be the meshsize of the partition \mathcal{T}_h .

Let $T \in \mathcal{T}_h$ be a polyhedral domain with boundary ∂T . We define the space of scalar-valued weak functions on T as follows

$$W(T) = \{v = \{v_0, v_h\} : v_0 \in L^p(T), v_h \in L^p(\partial T)\},\$$

where v_0 and v_b represent the values of v in the interior and on the boundary of T respectively. Similarly, the space of vector-valued weak functions on T is defined by

$$V(T) = \{ \mathbf{v} = \{ \mathbf{v}_0, \mathbf{v}_h \} : \mathbf{v}_0 \in [L^p(T)]^3, \mathbf{v}_h \in [L^p(\partial T)]^3 \}.$$

Let $P_j(T)$ be the polynomial space on T with total degree no more than j. Denote by n an unit outward normal direction on ∂T . For any $v \in W(T)$, the discrete weak gradient $\nabla_{w,j,T}v$ is defined as the unique vector-valued polynomial in $[P_j(T)]^3$ such that

$$(\nabla_{w,j,T}v,\boldsymbol{\varphi})_T = -(v_0,\nabla\cdot\boldsymbol{\varphi})_T + \langle v_b,\boldsymbol{\varphi}\cdot\boldsymbol{n}\rangle_{\partial T}, \quad \forall \boldsymbol{\varphi} \in [P_j(T)]^3. \tag{3.1}$$

Similarly, for any $v \in V(T)$, the discrete weak curl $\nabla_{w,j,T} \times v$ is defined as the unique vector-valued polynomial in $[P_j(T)]^3$ such that

$$(\nabla_{w,j,T} \times \boldsymbol{v}, \boldsymbol{\varphi})_T = (\boldsymbol{v}_0, \nabla \times \boldsymbol{\varphi})_T - (\boldsymbol{v}_b \times \boldsymbol{n}, \boldsymbol{\varphi})_{\partial T}, \quad \forall \, \boldsymbol{\varphi} \in [P_j(T)]^3. \tag{3.2}$$

For a given non-negative integer k, the finite element spaces are defined as follows

$$\mathbf{V}_h = {\{\mathbf{v} : \mathbf{v}|_T \in [P_k(T)]^3, \forall T \in \mathcal{T}_h\},}$$

$$S_h = \{\{s_0, s_b\}: s_0|_T \in P_k(T), s_b|_{\partial T} \in P_k(\partial T), \forall T \in \mathcal{T}_h, s_b|_{\Gamma_0} = 0, s_b|_{\Gamma_b} \text{ is a constant}\},$$

$$M_h = \{\{\varphi_0, \varphi_b\}: \ \varphi_0|_T \in P_k(T), \varphi_b|_{\partial T} \in P_k(\partial T), \forall T \in \mathcal{T}_h, \ \int_{\Omega} \varphi_0 = 0\},$$

$$\mathbf{W}_h = \{ \mathbf{\psi} = \{ \mathbf{\psi}_0, \mathbf{\psi}_b \} : \mathbf{\psi}_0 |_T \in [P_k(T)]^3, \mathbf{\psi}_b |_{\partial T} \in G_k(\partial T), \forall T \in \mathcal{T}_h, \mathbf{\psi}_b |_{\Gamma} = 0 \},$$

where $G_k(\partial T) := [P_k(\tau)]^3 \times \boldsymbol{n}_{\tau}$ is the space of polynomials of degree k in the tangent space of ∂T , and \boldsymbol{n}_{τ} denotes the unit outward normal vector on τ with $\tau \in \partial T$.

For simplicity of notation and without confusion, for any $\sigma \in S_h$ or $\sigma \in M_h$, denote by $\nabla_w \sigma$ the discrete weak gradient $\nabla_{w,k,T} \sigma$ computed by (3.1) on T, i.e.,

$$(\nabla_w \sigma)|_T = \nabla_{w,k,T}(\sigma|_T), \quad \forall \sigma \in S_h \text{ or } \sigma \in M_h.$$

Similarly, for any $\mathbf{q} \in \mathbf{W}_h$, denote by $\nabla_w \times \mathbf{q}$ the discrete weak curl $\nabla_{w,k,T} \times \mathbf{q}$ computed by (3.2) on T, i.e.,

$$(\nabla_w \times \boldsymbol{q})|_T = \nabla_{w,k,T} \times (\boldsymbol{q}|_T), \quad \forall \boldsymbol{q} \in \boldsymbol{W}_h.$$

With the discrete weak gradient and discrete weak curl, an approximation of the bilinear form $B(\cdot; \cdot)$ is thus given by

$$B_h(\boldsymbol{v}, r; \varphi, \boldsymbol{\psi}) = (v, \varepsilon \nabla_w \varphi + \nabla_w \times \boldsymbol{\psi}) + (\boldsymbol{\psi}_0, \varepsilon \nabla_w r), \forall (\boldsymbol{v}, r, \varphi, \boldsymbol{\psi}) \in \boldsymbol{V}_h \times S_h \times M_h \times \boldsymbol{W}_h. \tag{3.3}$$

Now we are ready to present the L^p -PDWG finite element method for the div-curl system (1.1a)-(1.1c).

Algorithm 1 (L^p -PDWG Algorithm). The L^p -PDWG finite element method for the div–curl system (1.1a)–(1.1c) seeks a $\boldsymbol{u}_h \in \boldsymbol{V}_h$, together with three auxiliary variables $s_h \in S_h$, $\lambda_h \in M_h$, $\boldsymbol{q}_h \in \boldsymbol{W}_h$, such that

$$\begin{cases}
s_1(\lambda_h, \mathbf{q}_h; \varphi, \boldsymbol{\psi}) + B_h(\mathbf{u}_h, s_h; \varphi, \boldsymbol{\psi}) &= F(\varphi, \boldsymbol{\psi}), & \forall \varphi \in M_h, \boldsymbol{\psi} \in \mathbf{W}_h, \\
-s_2(s_h, r) + B_h(\boldsymbol{v}, r; \lambda_h, \mathbf{q}_h) &= 0, & \forall \boldsymbol{v} \in \mathbf{V}_h, r \in S_h.
\end{cases}$$
(3.4)

Here $F(\cdot, \cdot)$ is given in Eq. (2.8), and the L^p stabilizer s_1 is defined by

$$s_1(\lambda_h, \boldsymbol{q}_h; \varphi, \boldsymbol{\psi}) = \rho_1 \sum_{T \in \mathcal{T}_h} \int_{\partial T} h_T^{1-p} |\lambda_0 - \lambda_b|^{p-1} sgn(\lambda_0 - \lambda_b)(\varphi_0 - \varphi_b) ds$$

$$+ \rho_2 \sum_{T \in \mathcal{T}_b} h_T^{1-p} \int_{\partial T} |\boldsymbol{q}_0 \times \boldsymbol{n} - \boldsymbol{q}_b \times \boldsymbol{n}|^{p-1} sgn(\boldsymbol{q}_0 \times \boldsymbol{n} - \boldsymbol{q}_b \times \boldsymbol{n}) (\boldsymbol{\psi}_0 \times \boldsymbol{n} - \boldsymbol{\psi}_b \times \boldsymbol{n}) ds,$$

and the L^q stabilizer s_2 is defined accordingly in the space M_h as follows

$$s_2(s_h; r) = \rho_3 \sum_{T \in \mathcal{T}_h} h_T^{1-q} \int_{\partial T} |s_0 - s_b|^{q-1} sgn(s_0 - s_b)(r_0 - r_b) ds,$$

where p > 1, q > 1 such that $\frac{1}{p} + \frac{1}{q} = 1$, $\rho_i > 0$ for i = 1, 2, 3 are parameters with values at user's discretion.

The above L^p -PDWG scheme (3.4) also offers an approximation of the normal ε -harmonic vector fields $\mathbb{W}_0^{\varepsilon n,p}$. Our later theoretical result (see Theorem 5.2) demonstrates that the difference $\eta_h = \mathcal{Q}_h \boldsymbol{u} - \boldsymbol{u}_h$ is sufficiently close to a true normal ε -harmonic vector field η . Here \mathcal{Q}_h denote the L^2 projection operator onto the finite element space \boldsymbol{V}_h , and \boldsymbol{u}_h is the solution of (3.4) for the div–curl system (1.1a)–(1.1c). Consequently, a vector field $\eta_h \in \boldsymbol{V}_h$ is said to be a discrete normal ε -harmonic function if there exists a vector field $\boldsymbol{u} \in W^{div_{\varepsilon},p}(\Omega) \cap W^{curl,p}(\Omega)$ satisfying $\eta_h = \mathcal{Q}_h \boldsymbol{u} - \boldsymbol{u}_h$.

4. Solution existence and uniqueness

This section is dedicated to the study of solution existence and uniqueness of the L^p -PDWG scheme (3.4). For simplicity, we assume that ε is piecewise constant with respect to the partition \mathcal{T}_h respectively. Note that all the results can be generalized to piecewise smooth ε without any difficulty.

We define the following two semi-norms; i.e.,

$$\|(\lambda_h, \boldsymbol{q}_h)\| = \left(s_1(\lambda_h, \boldsymbol{q}_h; \lambda_h, \boldsymbol{q}_h)\right)^{\frac{1}{p}}, \quad \lambda_h \in M_h, \quad \boldsymbol{q}_h \in \boldsymbol{W}_h,$$

$$(4.1)$$

$$|||s_h||| = \left(s_2(s_h; s_h)\right)^{\frac{1}{q}}, \quad s_h \in S_h.$$
(4.2)

Let Q_h be the projection operator onto the weak finite element space S_h or M_h such that

$$(Q_h w)|_T = \{Q_0 w|_T, Q_b w|_{\partial T}\},\,$$

where Q_0 and Q_b are the L^2 projection operators onto $P_k(T)$ and $P_k(\tau)$ on each face $\tau \in \partial T$. Similarly, denote by \mathbb{Q}_0 , \mathbb{Q}_b and \mathbb{Q}_h the L^2 projection operators onto $[P_k(T)]^3$, $G_k(\tau) = [P_k(\tau)]^3 \times \mathbf{n}_{\tau}$, and \mathbf{W}_h , respectively.

Lemma 4.1 ([26]). The L^2 projections Q_h and Q_h satisfy the commutative property

$$\nabla_w(Q_h w) = \mathcal{Q}_h(\nabla w), \qquad \forall w \in W^{1,p}(T), \tag{4.3}$$

$$\nabla_{w} \times (\mathbb{Q}_{h} \psi) = \mathcal{Q}_{h}(\nabla \times \psi), \qquad \forall \psi \in W^{curl,p}(T). \tag{4.4}$$

Theorem 4.2 ([14]). (Helmholtz Decomposition) For any vector-valued function $\mathbf{u} \in [L^p(\Omega)]^3$, there exists a unique $\boldsymbol{\psi} \in W_0^{\operatorname{curl},p}(\Omega)$, $\phi \in W^{1,p}(\Omega)/\mathbb{R}$, and $\boldsymbol{\eta} \in W_0^{\operatorname{sn},p}(\Omega)$ such that

$$\mathbf{u} = \varepsilon^{-1} \nabla \times \mathbf{v} + \nabla \phi + \mathbf{\eta}, \tag{4.5}$$

$$\nabla \cdot (\varepsilon \psi) = 0, \ \langle \varepsilon \psi \cdot \mathbf{n}_i, 1 \rangle_{\Gamma_i} = 0, \ i = 1, \dots, L. \tag{4.6}$$

In addition, there holds

$$\|\boldsymbol{\psi}\|_{W^{\operatorname{curl},p}(\Omega)} + \|\nabla\phi\|_{L^{p}(\Omega)} \lesssim \|\varepsilon^{\frac{1}{p}}\boldsymbol{u}\|_{L^{p}(\Omega)}. \tag{4.7}$$

Theorem 4.3. The kernel of the matrix of the L^p -PDWG method (3.4) is given by

$$K_h = \{(\boldsymbol{v}_h, s_h = 0, \lambda_h = 0, \boldsymbol{q}_h = 0) : \boldsymbol{v}_h \in \boldsymbol{V}_h \cap \mathbb{W}_0^{\varepsilon n, p}(\Omega)\}.$$

In other words, the kernel of the matrix of the L^p -PDWG scheme (3.4) is isomorphic to the subspace of $\mathbb{W}_0^{\varepsilon n,p}(\Omega)$ consisting of harmonic functions that are piecewise polynomial of degree k.

Proof. Let $(\boldsymbol{u}_h^{(1)}, s_h^{(1)}, \lambda_h^{(1)}, \boldsymbol{q}_h^{(1)})$ and $(\boldsymbol{u}_h^{(2)}, s_h^{(2)}, \lambda_h^{(2)}, \boldsymbol{q}_h^{(2)})$ be two different solutions of (3.4). This gives, for i = 1, 2,

$$s_1(\lambda_h^{(i)}, \boldsymbol{q}_h^{(i)}; \varphi, \boldsymbol{\psi}) + B_h(\boldsymbol{u}_h^{(i)}, s_h^{(i)}; \varphi, \boldsymbol{\psi}) = F(\varphi, \boldsymbol{\psi}), \quad \forall \varphi \in M_h, \ \boldsymbol{\psi} \in \boldsymbol{W}_h,$$

$$(4.8)$$

$$-s_2(s_h^{(i)}, r) + B_h(\mathbf{v}, r; \lambda_h^{(i)}, \mathbf{q}_h^{(i)}) = 0, \quad \forall \mathbf{v} \in \mathbf{V}_h, \ r \in S_h.$$
(4.9)

Given any i = 1, 2, taking $(\varphi, \psi) = (\lambda_h^{(j)}, \mathbf{q}_h^{(j)})$ in (4.8) and using (4.9), we easily get

$$s_1(\lambda_h^{(i)}, \boldsymbol{q}_h^{(i)}; \lambda_h^{(j)}, \boldsymbol{q}_h^{(j)}) + s_2(s_h^{(j)}, s_h^{(i)}) = F(\lambda_h^{(j)}, \boldsymbol{q}_h^{(j)}), \quad \forall i, j = 1, 2.$$

$$(4.10)$$

Consequently, for j = 1, 2,

$$s_1(\lambda_h^{(1)}, \boldsymbol{q}_h^{(1)}; \lambda_h^{(j)}, \boldsymbol{q}_h^{(j)}) + s_2(s_h^{(j)}, s_h^{(1)}) = s_1(\lambda_h^{(2)}, \boldsymbol{q}_h^{(2)}; \lambda_h^{(j)}, \boldsymbol{q}_h^{(j)}) + s_2(s_h^{(j)}, s_h^{(2)}). \tag{4.11}$$

Choosing j=1 in (4.11) and using the Young's inequality $|AB| \leq \frac{|A|^p}{p} + \frac{|B|^q}{q}$ yields that

$$\begin{split} s_1(\lambda_h^{(1)}, \boldsymbol{q}_h^{(1)}; \lambda_h^{(1)}, \boldsymbol{q}_h^{(1)}) + s_2(s_h^{(1)}, s_h^{(1)}) &\leq \frac{s_1(\lambda_h^{(2)}, \boldsymbol{q}_h^{(2)}; \lambda_h^{(2)}, \boldsymbol{q}_h^{(2)})}{p} \\ &+ \frac{s_1(\lambda_h^{(1)}, \boldsymbol{q}_h^{(1)}; \lambda_h^{(1)}, \boldsymbol{q}_h^{(1)})}{q} + \frac{s_2(s_h^{(1)}, s_h^{(1)})}{q} + \frac{s_2(s_h^{(2)}, s_h^{(2)})}{p}, \end{split}$$

which leads to

$$s_1(\lambda_h^{(1)}, \boldsymbol{q}_h^{(1)}; \lambda_h^{(1)}, \boldsymbol{q}_h^{(1)}) + s_2(s_h^{(1)}, s_h^{(1)}) \le s_1(\lambda_h^{(2)}, \boldsymbol{q}_h^{(2)}; \lambda_h^{(2)}, \boldsymbol{q}_h^{(2)}) + s_2(s_h^{(2)}, s_h^{(2)}).$$

Similarly, we take i = 2 in (4.11) and use the Young's inequality again to derive

$$s_1(\lambda_h^{(2)}, \boldsymbol{q}_h^{(2)}; \lambda_h^{(2)}, \boldsymbol{q}_h^{(2)}) + s_2(s_h^{(2)}, s_h^{(2)}) \le s_1(\lambda_h^{(1)}, \boldsymbol{q}_h^{(1)}; \lambda_h^{(1)}, \boldsymbol{q}_h^{(1)}) + s_2(s_h^{(1)}, s_h^{(1)}).$$

Combining the last two inequality leads to

$$s_1(\lambda_h^{(1)}, \boldsymbol{q}_h^{(1)}; \lambda_h^{(1)}, \boldsymbol{q}_h^{(1)}) + s_2(s_h^{(1)}, s_h^{(1)}) = s_1(\lambda_h^{(2)}, \boldsymbol{q}_h^{(2)}; \lambda_h^{(2)}, \boldsymbol{q}_h^{(2)}) + s_2(s_h^{(2)}, s_h^{(2)}). \tag{4.12}$$

Note that for any two real numbers A and B, there holds

$$\left|\frac{A+B}{2}\right|^p \le \frac{|A|^p + |B|^p}{2},$$

and the equality holds true if and only if A = B. This follows that

$$s_{1}\left(\frac{\lambda_{h}^{(1)} + \lambda_{h}^{(2)}}{2}, \frac{\boldsymbol{q}_{h}^{(1)} + \boldsymbol{q}_{h}^{(2)}}{2}; \frac{\lambda_{h}^{(1)} + \lambda_{h}^{(2)}}{2}, \frac{\boldsymbol{q}_{h}^{(1)} + \boldsymbol{q}_{h}^{(2)}}{2}\right) + s_{2}\left(\frac{s_{h}^{(1)} + s_{h}^{(2)}}{2}, \frac{s_{h}^{(1)} + s_{h}^{(2)}}{2}\right) \\ \leq \frac{1}{2}\left(s_{1}(\lambda_{h}^{(1)}, \boldsymbol{q}_{h}^{(1)}; \lambda_{h}^{(1)}, \boldsymbol{q}_{h}^{(1)}) + s_{1}(\lambda_{h}^{(2)}, \boldsymbol{q}_{h}^{(2)}; \lambda_{h}^{(2)}, \boldsymbol{q}_{h}^{(2)})\right) + \frac{1}{2}\left(s_{2}(s_{h}^{(1)}, s_{h}^{(1)}) + s_{2}(s_{h}^{(2)}, s_{h}^{(2)})\right).$$

$$(4.13)$$

On the other hand, a direct calculation from (4.11)-(4.12) yields

$$\begin{split} &s_{1}(\lambda_{h}^{(1)},\boldsymbol{q}_{h}^{(1)};\lambda_{h}^{(1)},\boldsymbol{q}_{h}^{(1)})+s_{2}(s_{h}^{(1)},s_{h}^{(1)})\\ &=\frac{1}{2}\Big(s_{1}(\lambda_{h}^{(1)},\boldsymbol{q}_{h}^{(1)};\lambda_{h}^{(1)},\boldsymbol{q}_{h}^{(1)})+s_{2}(s_{h}^{(1)},s_{h}^{(1)})+s_{1}(\lambda_{h}^{(2)},\boldsymbol{q}_{h}^{(2)};\lambda_{h}^{(1)},\boldsymbol{q}_{h}^{(1)})+s_{2}(s_{h}^{(1)},s_{h}^{(2)})\Big)\\ &=s_{1}(\frac{\lambda_{h}^{(1)}+\lambda_{h}^{(2)}}{2},\frac{\boldsymbol{q}_{h}^{(1)}+\boldsymbol{q}_{h}^{(2)}}{2};\lambda_{h}^{(1)},\boldsymbol{q}_{h}^{(1)})+s_{2}(s_{h}^{(1)},\frac{s_{h}^{(1)}+s_{h}^{(2)}}{2}). \end{split}$$

Using the Young's inequality again, we get

$$\begin{split} &s_1(\lambda_h^{(1)}, \boldsymbol{q}_h^{(1)}; \lambda_h^{(1)}, \boldsymbol{q}_h^{(1)}) + s_2(s_h^{(1)}, s_h^{(1)}) \\ \leq &s_1(\frac{\lambda_h^{(1)} + \lambda_h^{(2)}}{2}, \frac{\boldsymbol{q}_h^{(1)} + \boldsymbol{q}_h^{(2)}}{2}; \frac{\lambda_h^{(1)} + \lambda_h^{(2)}}{2}, \frac{\boldsymbol{q}_h^{(1)} + \boldsymbol{q}_h^{(2)}}{2}) + s_2(\frac{s_h^{(1)} + s_h^{(2)}}{2}, \frac{s_h^{(1)} + s_h^{(2)}}{2}). \end{split}$$

Then we conclude from (4.13) and (4.12)

$$s_{1}(\frac{\lambda_{h}^{(1)} + \lambda_{h}^{(2)}}{2}, \frac{\boldsymbol{q}_{h}^{(1)} + \boldsymbol{q}_{h}^{(2)}}{2}; \frac{\lambda_{h}^{(1)} + \lambda_{h}^{(2)}}{2}, \frac{\boldsymbol{q}_{h}^{(1)} + \boldsymbol{q}_{h}^{(2)}}{2}) + s_{2}(\frac{s_{h}^{(1)} + s_{h}^{(2)}}{2}, \frac{s_{h}^{(1)} + s_{h}^{(2)}}{2})$$

$$= s_{1}(\lambda_{h}^{(1)}, \boldsymbol{q}_{h}^{(1)}; \lambda_{h}^{(1)}, \boldsymbol{q}_{h}^{(1)}) + s_{2}(s_{h}^{(1)}, s_{h}^{(1)}) = s_{1}(\lambda_{h}^{(2)}, \boldsymbol{q}_{h}^{(2)}; \lambda_{h}^{(2)}, \boldsymbol{q}_{h}^{(2)}) + s_{2}(s_{h}^{(2)}, s_{h}^{(2)}).$$

The above equation holds true if and only if

$$\lambda_0^{(1)} - \lambda_b^{(1)} = \lambda_0^{(2)} - \lambda_b^{(2)}, \quad \text{on } \partial T,$$
 (4.14)

$$\mathbf{q}_{0}^{(1)} \times \mathbf{n} - \mathbf{q}_{b}^{(1)} \times \mathbf{n} = \mathbf{q}_{0}^{(2)} \times \mathbf{n} - \mathbf{q}_{b}^{(2)} \times \mathbf{n}, \quad \text{on } \partial T,$$
 (4.15)

$$s_0^{(1)} - s_b^{(1)} = s_0^{(2)} - s_b^{(2)}, \quad \text{on } \partial T,$$
(4.16)

Denoting $\epsilon_h = \lambda_h^{(1)} - \lambda_h^{(2)} = \{\epsilon_0, \epsilon_b\}$, $\mathbf{e}_h = \mathbf{q}_h^{(1)} - \mathbf{q}_h^{(2)} = \{\mathbf{e}_0, \mathbf{e}_b\}$, $e_h = s_h^{(1)} - s_h^{(2)} = \{e_0, e_b\}$, we have

$$\epsilon_0 = \epsilon_b$$
, on ∂T , $\mathbf{e}_0 \times \mathbf{n} = \mathbf{e}_b \times \mathbf{n}$, on ∂T , $e_0 = e_b$, on ∂T . (4.17)

Since $s_0^{(1)} - s_b^{(1)} = s_0^{(2)} - s_b^{(2)}$ on ∂T , there holds

$$s_2(s_h^{(1)}, r) = s_2(s_h^{(2)}, r), \quad \forall r \in S_h,$$

which, combined with (4.9), gives

$$B_h(\boldsymbol{v}, r; \lambda_h^{(1)}, \boldsymbol{q}_h^{(1)}) = B_h(\boldsymbol{v}, r; \lambda_h^{(2)}, \boldsymbol{q}_h^{(2)}), \quad \forall \boldsymbol{v} \in \boldsymbol{V}_h, r \in S_h,$$

or equivalently,

$$B_h(\boldsymbol{v}, r; \epsilon_h, \mathbf{e}_h) = 0, \quad \forall \boldsymbol{v} \in \mathbf{V}_h, r \in S_h,$$

i.e.,

$$(\mathbf{e}_0, \varepsilon \nabla_w r) + (\mathbf{v}, \varepsilon \nabla_w \epsilon_h + \nabla_w \times \mathbf{e}_h) = 0, \quad \forall \mathbf{v} \in \mathbf{V}_h, r \in S_h. \tag{4.18}$$

It follows from (4.17) that $\epsilon_0 \in C(\Omega)$, $e_0 \in C(\Omega)$ and $\mathbf{e}_0 \in H_0(curl; \Omega)$, which indicates

$$\nabla \epsilon_0 = \nabla_w \epsilon_h, \ \nabla \times \mathbf{e}_0 = \nabla_w \times \mathbf{e}_h. \tag{4.19}$$

Letting r = 0 and varying v in (4.18), we get

$$\varepsilon \nabla_w \epsilon_h + \nabla_w \times \mathbf{e}_h = 0$$
,

which, together with (4.19), gives

$$\varepsilon \nabla \epsilon_0 + \nabla \times \mathbf{e}_0 = 0. \tag{4.20}$$

Using $\mathbf{e}_0 \in H_0(curl; \Omega)$, we have

$$(\varepsilon \nabla \epsilon_0 + \nabla \times \mathbf{e}_0, \nabla \epsilon_0) = (\varepsilon \nabla \epsilon_0, \nabla \epsilon_0) + (\nabla \times \mathbf{e}_0, \nabla \epsilon_0)$$
$$= (\varepsilon \nabla \epsilon_0, \nabla \epsilon_0) + \langle \mathbf{n} \times \mathbf{e}_0, \epsilon_0 \rangle = (\varepsilon \nabla \epsilon_0, \nabla \epsilon_0),$$

which, from (4.20), implies $\nabla \epsilon_0 = \mathbf{0}$, and hence $\epsilon_0 \equiv 0$ as a function with mean value 0. This further leads to $\epsilon_b \equiv 0$. Thus, from (4.20) we have

$$\nabla \times \mathbf{e}_0 = 0$$
, in Ω .

Note that \mathbf{e}_0 satisfies

$$(\mathbf{e}_0, \varepsilon \nabla_w r) = 0, \quad \forall r \in S_h.$$

This leads to $\mathbf{e}_0 \in H(div_{\varepsilon}; \Omega)$ and

$$\nabla \cdot (\varepsilon \mathbf{e}_0) = 0, \quad \langle \mathbf{e}_0 \cdot \mathbf{n}_i, 1 \rangle_{\Gamma_i} = 0, i = 1, 2, \dots, L.$$

This, together with $\nabla \times \mathbf{e}_0 = 0$ and $\mathbf{e}_0 \in H_0(curl; \Omega)$, indicates that $\mathbf{e}_0 \equiv 0$, and further $\mathbf{e}_b = \mathbf{n} \times (\mathbf{e}_b \times \mathbf{n}) = \mathbf{n} \times 0 = 0$. Using (4.14)–(4.16), we have

$$s_1(\lambda_h^{(1)}, \boldsymbol{q}_h^{(1)}; \varphi, \boldsymbol{\psi}) = s_1(\lambda_h^{(2)}, \boldsymbol{q}_h^{(2)}; \varphi, \boldsymbol{\psi}),$$

which yields, together with (4.8),

$$B_h(\mathbf{u}_h^{(1)}, s_h^{(1)}; \varphi, \psi) = B_h(\mathbf{u}_h^{(2)}, s_h^{(2)}; \varphi, \psi), \quad \forall \varphi \in M_h, \ \psi \in \mathbf{W}_h.$$

Denote $\mathbf{e}_{\mathbf{u}_h} = \mathbf{u}_h^{(1)} - \mathbf{u}_h^{(2)}$. The above equality is equivalent to

$$0 = B_h(\mathbf{e}_{\mathbf{u}_h}, e_h; \varphi, \psi) = (\mathbf{e}_{\mathbf{u}_h}, \varepsilon \nabla_w \varphi + \nabla_w \times \psi) + (\psi_0, \varepsilon \nabla_w e_h), \quad \forall \varphi \in M_h, \ \psi \in \mathbf{W}_h.$$

$$(4.21)$$

Now we have, from the Helmholtz decomposition (4.5),

$$\mathbf{e}_{\mathbf{u}_{b}} = \varepsilon^{-1} \nabla \times \tilde{\boldsymbol{\psi}} + \nabla \tilde{\boldsymbol{\phi}} + \tilde{\boldsymbol{\eta}},$$

where $\tilde{\eta} \in \mathbb{W}_0^{\varepsilon n,p}(\Omega)$ and $\tilde{\psi} \in W_0^{\operatorname{curl},p}(\Omega)$ satisfying $\nabla \cdot (\varepsilon \tilde{\psi}) = 0$ and $\langle \varepsilon \tilde{\psi} \cdot \boldsymbol{n}_i, 1 \rangle_{\Gamma_i} = 0$ for $i = 1, \ldots, L$. It follows from $e_0 = e_b$ on ∂T for each element $T \in \mathcal{T}_h$ that $e_0 \in W^{1,p}(\Omega)$. This leads to $\nabla_w e_h = \nabla e_0$. If the dimension of $\mathbb{W}_0^{\varepsilon n,p}(\Omega)$ is 0, we have $\tilde{\eta} = 0$. Letting the test functions ϕ and ψ in (4.21) be the L^2 projections of the corresponding function in the Helmholtz decomposition gives rise to

$$0 = (\mathbf{e}_{\mathbf{u}_{h}}, \varepsilon \nabla_{w} Q_{h} \tilde{\varphi} + \nabla_{w} \times \mathbb{Q}_{h} \tilde{\psi}) + (\mathbb{Q}_{0} \tilde{\psi}, \varepsilon \nabla_{w} e_{h})$$

$$= (\mathbf{e}_{\mathbf{u}_{h}}, \mathcal{Q}_{h} \varepsilon \nabla \tilde{\varphi} + \mathcal{Q}_{h} \nabla \times \tilde{\psi}) + (\tilde{\psi}, \varepsilon \nabla e_{0})$$

$$= (\mathbf{e}_{\mathbf{u}_{h}}, \varepsilon \nabla \tilde{\varphi} + \nabla \times \tilde{\psi}) + (\tilde{\psi}, \varepsilon \nabla e_{0})$$

$$= (\varepsilon \mathbf{e}_{\mathbf{u}_{h}}, \mathbf{e}_{\mathbf{u}_{h}} - \tilde{\eta}) + (\tilde{\psi}, \varepsilon \nabla e_{0})$$

$$= (\varepsilon \mathbf{e}_{\mathbf{u}_{h}}, -\tilde{\eta}), \mathbf{e}_{\mathbf{u}_{h}} - \tilde{\eta}),$$

$$(4.22)$$

which leads to $\mathbf{e}_{u_h} - \tilde{\eta} = 0$, i.e., \mathbf{e}_{u_h} is a harmonic function. As a harmonic function in the form of piecewise polynomial of degree k, the first term on the right-hand side of (4.21) is zero for any test functions $\varphi \in M_h$ and $\psi \in \mathbf{W}_h$, which further implies that $\nabla_w e_h = 0$. Using (4.17) gives $\nabla e_0 = \nabla_w e_h = 0$. Therefore we obtain $e_0 \equiv 0$ and further $e_b \equiv 0$.

This completes the proof of the theorem. \Box

Our main result for the solution existence and uniqueness of the numerical scheme (3.4) is stated as follows.

Theorem 4.4. The L^p -PDWG finite element scheme (3.4) has a unique solution for s_h , λ_h and \mathbf{q}_h . The solution \mathbf{u}_h is unique up to a harmonic function $\boldsymbol{\eta}_h \in \mathbb{W}_0^{en,p}(\Omega)$ which is a piecewise polynomial of degree k.

Remark 4.5. For the lowest order k=0 of the L^p -PDWG scheme (3.4), any η_h in the kernel K_h of the matrix of the L^p -PDWG method is a piecewise constant vector field. η_h is thus continuous across each interior element interface and has vanishing value on the domain boundary along the normal direction. This leads to $\eta_h \equiv 0$. Therefore, the L^p -PDWG finite element scheme (3.4) has a unique solution for \boldsymbol{u}_h in the case of the lowest order element.

5. L^q -Error analysis for the primal variable

In this section, we shall establish the L^q error estimates for primal variable \boldsymbol{u}_h in the L^p -PDWG scheme (3.4). Denote the error functions by

$$e_{\mathbf{u}} = \mathcal{Q}_h \mathbf{u} - \mathbf{u}_h, \ e_s = Q_h s - s_h, \ e_{\lambda} = Q_h \lambda - \lambda_h, \ e_{\mathbf{q}} = \mathbb{Q}_h \mathbf{q} - \mathbf{q}_h.$$

We begin with the study of error equations for the L^p -PDWG scheme (3.4) developed for the div-curl system (1.1a)–(1.1c).

5.1. Error equations

For the exact solution $\{u; s = 0\}$ of the div-curl system, recalling the definition of $B_h(\cdot; \cdot)$ in (3.3) and using (3.1) and (3.2), we have

$$B_{h}(Q_{h}\mathbf{u}, Q_{h}\mathbf{s}; \varphi, \boldsymbol{\psi}) = (Q_{h}\mathbf{u}, \varepsilon\nabla\varphi_{0} + \nabla\times\boldsymbol{\psi}_{0}) + \langle Q_{h}\mathbf{u}, \varepsilon\mathbf{n}(\varphi_{b} - \varphi_{0}) + (\boldsymbol{\psi}_{0} - \boldsymbol{\psi}_{b})\times\mathbf{n}\rangle_{\varepsilon_{h}}$$
$$= (\mathbf{u}, \varepsilon\nabla\varphi_{0} + \nabla\times\boldsymbol{\psi}_{0}) + \langle Q_{h}\mathbf{u}, \varepsilon\mathbf{n}(\varphi_{b} - \varphi_{0}) + (\boldsymbol{\psi}_{0} - \boldsymbol{\psi}_{b})\times\mathbf{n}\rangle_{\varepsilon_{h}}.$$

By using the integration by parts and (1.1a)–(1.1c), we easily obtain

$$B_{h}(Q_{h}\mathbf{u}, Q_{h}\mathbf{s}; \varphi, \mathbf{\psi})$$

$$= -(\nabla \cdot (\varepsilon \mathbf{u}), \varphi_{0}) + (\nabla \times \mathbf{u}, \mathbf{\psi}_{0}) + \langle \mathbf{u}, \varepsilon \mathbf{n}(\varphi_{0} - \varphi_{b}) + (\mathbf{\psi}_{b} - \mathbf{\psi}_{0}) \times \mathbf{n} \rangle_{\varepsilon_{h}}$$

$$+ \langle Q_{h}\mathbf{u}, \varepsilon \mathbf{n}(\varphi_{b} - \varphi_{0}) + (\mathbf{\psi}_{0} - \mathbf{\psi}_{b}) \times \mathbf{n} \rangle_{\varepsilon_{h}} + \langle \phi_{1}, \varphi_{b} \rangle_{\partial \Omega}$$

$$= \langle \phi_{1}, \varphi_{b} \rangle_{\partial \Omega} - (f, \varphi_{0}) + (\mathbf{g}, \mathbf{\psi}_{0}) + \langle \mathbf{u} - Q_{h}\mathbf{u}, \varepsilon \mathbf{n}(\varphi_{0} - \varphi_{b}) + (\mathbf{\psi}_{b} - \mathbf{\psi}_{0}) \times \mathbf{n} \rangle_{\varepsilon_{h}}.$$

Noticing that $\lambda = 0$ and $\mathbf{q} = 0$, then

$$s_1(e_{\lambda}, e_{\mathbf{q}}; \varphi, \psi) + B_h(e_{\mathbf{u}}, e_{\mathbf{s}}; \varphi, \psi) = \langle \mathbf{u} - \mathcal{Q}_h \mathbf{u}, \varepsilon \mathbf{n}(\varphi_0 - \varphi_b) + (\psi_b - \psi_0) \times \mathbf{n} \rangle_{\mathcal{E}_h}. \tag{5.1}$$

Similarly, we conclude from the fact s = 0, q = 0, $\lambda = 0$ that

$$-s_2(e_s, r) + B_h(v, r; e_\lambda, e_a) = 0. (5.2)$$

The above two Eqs. (5.1)–(5.2) are the error equations for the L^p -PDWG scheme (3.4), which will be frequently used in our error estimates.

5.2. Error estimates for the dual variables

Recall that \mathcal{T}_h is a shape-regular finite element partition of the domain Ω . For any $T \in \mathcal{T}_h$ and $\nabla w \in L^q(T)$ with q > 1, the following trace inequality holds true:

$$\|w\|_{L^{q}(\partial T)}^{q} \le Ch_{T}^{-1} \Big(\|w\|_{L^{q}(T)}^{q} + h_{T}^{q} \|\nabla w\|_{L^{q}(T)}^{q} \Big). \tag{5.3}$$

By using the Cauchy-Schwarz inequality and the trace inequality, we get

$$|\langle w, v \rangle_{\mathcal{E}_{h}}| \leq \left(\sum_{T \in \mathcal{T}_{h}} \|w\|_{L^{q}(\partial T)}^{q}\right)^{\frac{1}{q}} \left(\sum_{T \in \mathcal{T}_{h}} \|v\|_{L^{p}(\partial T)}^{p}\right)^{\frac{1}{p}}$$

$$\leq Ch^{-\frac{1}{q}} (\|w\|_{L^{q}(T)} + h\|\nabla w\|_{L^{q}(T)}) \left(\sum_{T \in \mathcal{T}_{h}} \|v\|_{L^{p}(\partial T)}^{p}\right)^{\frac{1}{p}}.$$

$$(5.4)$$

Now we are ready to present the error estimates for the dual variables.

Theorem 5.1. Assume the solution of the div–curl system (1.1a)–(1.1c) satisfies $\mathbf{u} \in [W^{k+\theta,q}(\Omega)]^3$ for $\theta \in (1/2, 1]$. For the numerical solution \mathbf{u}_h , s_h , λ_h , \mathbf{q}_h arising from the L^p -PDWG scheme (3.4), there holds

$$\|(\boldsymbol{e}_{\lambda}, \boldsymbol{e}_{\boldsymbol{q}})\| \leq C h^{(k+\theta)\frac{q}{p}} \|\nabla^{k+\theta} \boldsymbol{u}\|_{L^{q}(\Omega)}^{\frac{q}{p}}, \tag{5.5}$$

$$|||e_s||| \le Ch^{(k+\theta)}||\nabla^{k+\theta}\boldsymbol{u}||_{L^q(\Omega)}. \tag{5.6}$$

Proof. First, we have, from the error Eqs. (5.1)–(5.2) that

$$s_1(e_{\lambda}, e_{\mathbf{q}}; e_{\lambda}, e_{\mathbf{q}}) + s_2(e_s, e_s) = \langle \mathbf{u} - \mathcal{Q}_h \mathbf{u}, \varepsilon \mathbf{n}(e_{\lambda,0} - e_{\lambda,b}) + (e_{\mathbf{q},b} - e_{\mathbf{q},0}) \times \mathbf{n} \rangle \varepsilon_h. \tag{5.7}$$

In light of (5.4) and using the approximation property of Q_h , we get

$$|\langle \mathbf{u} - \mathcal{Q}_h \mathbf{u}, \varepsilon \mathbf{n}(e_{\lambda,0} - e_{\lambda,b}) + (e_{\mathbf{q},b} - e_{\mathbf{q},0}) \times \mathbf{n} \rangle_{\mathcal{E}_h}|$$

$$\leq Ch^{k+\theta-\frac{1}{q}} \|\nabla^{k+\theta} \mathbf{u}\|_{L^{q}} \left(\sum_{T \in \mathcal{T}_{b}} (\|\varepsilon \mathbf{n}(e_{\lambda,0} - e_{\lambda,b})\|_{L^{p}(\partial T)}^{p} + \|(e_{\mathbf{q},b} - e_{\mathbf{q},0}) \times \mathbf{n}\|_{L^{p}(\partial T)}^{p}) \right)^{\frac{1}{p}}$$

$$(5.8)$$

$$\leq Ch^{k+\theta} \|\nabla^{k+\theta} \boldsymbol{u}\|_{L^q} \|(\boldsymbol{e}_{\lambda}, \boldsymbol{e}_{\boldsymbol{q}})\|.$$

Substituting the above inequality into (5.7) and using the Cauchy-Schwarz inequality yields

$$\|(e_{\lambda}, e_{\mathbf{q}})\|^{p} + \|e_{s}\|^{q} \le C_{1} h^{(k+\theta)q} \|\nabla^{k+\theta} \mathbf{u}\|_{L^{q}(\Omega)}^{q}. \tag{5.9}$$

Then (5.5)–(5.6) follow directly. \square

5.3. L^q Error estimates for the primal variable \mathbf{u}_h

To derive the L^q -estimate for the error function e_u , we need employ the Helmholtz decomposition (4.5) for any function v, such that

$$\mathbf{v} = \varepsilon^{-1} \nabla \times \tilde{\mathbf{\psi}} + \nabla \tilde{\boldsymbol{\phi}} + \tilde{\boldsymbol{\eta}},\tag{5.10}$$

where $\tilde{\phi} \in W^{1,p}(\Omega)$, $\tilde{\psi} \in W_0^{curl,p}(\Omega)$, and $\tilde{\eta} \in \mathbb{W}_0^{\varepsilon n,p}(\Omega)$. We assume the $W^{\alpha,p}$ -regularity holds true for some fixed $\alpha \in (1/2, 1]$:

$$\|\tilde{\psi}\|_{\alpha,p} + \|\tilde{\phi}\|_{\alpha,p} \le C\|v - \tilde{\eta}\|_{0,p}. \tag{5.11}$$

The main convergence result of this paper is stated as follows.

Theorem 5.2. Let \boldsymbol{u} be a solution of the div–curl system (1.1a)–(1.1c) such that $\boldsymbol{u} \in [W^{k+\theta,q}(\Omega)]^3$ for $\theta \in (1/2, 1]$. Assume that the Helmholtz decomposition (5.10) has the $W^{\alpha,p}$ -regularity estimate (5.11). For a numerical solution \boldsymbol{u}_h , s_h , λ_h , \boldsymbol{q}_h arising from L^p -PDWG scheme (3.4), there exists a harmonic function $\tilde{\boldsymbol{\eta}} \in \mathbb{W}_0^{\varepsilon n,p}(\Omega)$ such that

$$\|\varepsilon^{\frac{1}{q}}(\boldsymbol{u}_{h}+\tilde{\boldsymbol{\eta}}-Q_{h}\boldsymbol{u})\|_{L^{q}(\Omega)} \leq Ch^{k+\theta+\alpha-1}\|\nabla^{k+\theta}\boldsymbol{u}\|_{L^{q}(\Omega)}. \tag{5.12}$$

Proof. Given any function \mathbf{v} , let $\tilde{\phi} \in W^{1,p}(\Omega)$, $\tilde{\boldsymbol{\psi}} \in W_0^{curl,p}(\Omega)$, and $\tilde{\boldsymbol{\eta}} \in \mathbb{W}_0^{\varepsilon n,p}(\Omega)$ satisfy (5.10). Taking $\varphi = Q_h \tilde{\boldsymbol{\phi}}$ and $\boldsymbol{\psi} = Q_h \tilde{\boldsymbol{\psi}}$ in $B_h(e_{\boldsymbol{u}}, e_s; \varphi, \boldsymbol{\psi})$ and using Lemma 4.1 gives

$$B_{h}(e_{\mathbf{u}}, e_{s}; \varphi, \boldsymbol{\psi}) = (e_{\mathbf{u}}, \varepsilon \nabla_{w} Q_{h} \tilde{\boldsymbol{\phi}} + \nabla_{w} \times \mathbb{Q}_{h} \tilde{\boldsymbol{\psi}}) + (\mathbb{Q}_{0} \tilde{\boldsymbol{\psi}}, \varepsilon \nabla_{w} e_{s})$$

$$= (e_{\mathbf{u}}, \varepsilon Q_{h} \nabla_{w} \tilde{\boldsymbol{\phi}} + Q_{h} \nabla_{w} \times \tilde{\boldsymbol{\psi}}) + (\mathbb{Q}_{0} \tilde{\boldsymbol{\psi}}, \varepsilon \nabla_{w} e_{s})$$

$$= (e_{\mathbf{u}}, \varepsilon \nabla \tilde{\boldsymbol{\phi}} + \nabla \times \tilde{\boldsymbol{\psi}}) + (\mathbb{Q}_{0} \tilde{\boldsymbol{\psi}}, \varepsilon \nabla_{w} e_{s}).$$

By using the Helmholtz decomposition (5.10), we have

$$B_{h}(e_{\mathbf{u}}, e_{s}; \varphi, \psi) = (\varepsilon e_{\mathbf{u}}, \mathbf{v} - \tilde{\mathbf{\eta}}) + (\varepsilon \mathbb{Q}_{0} \tilde{\mathbf{\psi}}, \nabla_{w} e_{s})$$

$$= (\varepsilon (e_{\mathbf{u}} - \tilde{\mathbf{\eta}}), \mathbf{v} - \tilde{\mathbf{\eta}}) + (\varepsilon \mathbb{Q}_{0} \tilde{\mathbf{\psi}}, \nabla_{w} e_{s}).$$
(5.13)

From the definition of the weak gradient, we have

$$\begin{split} (\varepsilon\mathbb{Q}_{0}\tilde{\boldsymbol{\psi}},\nabla_{w}e_{s}) = & (\varepsilon\mathbb{Q}_{0}\tilde{\boldsymbol{\psi}},\nabla e_{s,0}) + \langle \varepsilon\mathbb{Q}_{0}\tilde{\boldsymbol{\psi}}\cdot\boldsymbol{n},e_{s,b} - e_{s,0}\rangle_{\mathcal{E}_{h}} \\ = & (\varepsilon\tilde{\boldsymbol{\psi}},\nabla e_{s,0}) + \langle \varepsilon\mathbb{Q}_{0}\tilde{\boldsymbol{\psi}}\cdot\boldsymbol{n},e_{s,b} - e_{s,0}\rangle_{\mathcal{E}_{h}} \\ = & - (\nabla\cdot(\varepsilon\tilde{\boldsymbol{\psi}}),e_{s,0}) + \langle \varepsilon\tilde{\boldsymbol{\psi}}\cdot\boldsymbol{n},e_{s,0}\rangle_{\mathcal{E}_{h}} + \langle \varepsilon\mathbb{Q}_{0}\tilde{\boldsymbol{\psi}}\cdot\boldsymbol{n},e_{s,b} - e_{s,0}\rangle_{\mathcal{E}_{h}} \\ = & \langle \varepsilon\tilde{\boldsymbol{\psi}}\cdot\boldsymbol{n},e_{s,0} - e_{s,b}\rangle_{\mathcal{E}_{h}} + \langle \varepsilon\mathbb{Q}_{0}\tilde{\boldsymbol{\psi}}\cdot\boldsymbol{n},e_{s,b} - e_{s,0}\rangle_{\mathcal{E}_{h}} \\ = & \langle \varepsilon(\tilde{\boldsymbol{\psi}} - \mathbb{Q}_{0}\tilde{\boldsymbol{\psi}})\cdot\boldsymbol{n},e_{s,0} - e_{s,b}\rangle_{\mathcal{E}_{h}}. \end{split}$$

Substituting the above into 5.2 yields

$$(\varepsilon(e_{\mathbf{u}} - \tilde{\boldsymbol{\eta}}), \mathbf{v} - \tilde{\boldsymbol{\eta}}) = B(e_{\mathbf{u}}, e_{s}; \varphi, \boldsymbol{\psi}) - \langle \varepsilon(\tilde{\boldsymbol{\psi}} - \mathbb{Q}_{0}\tilde{\boldsymbol{\psi}}) \cdot \mathbf{n}, e_{s,0} - e_{s,b} \rangle_{\mathcal{E}_{h}}$$

$$= \langle \mathbf{u} - \mathcal{Q}_{h}\mathbf{u}, \varepsilon \mathbf{n}(\varphi_{0} - \varphi_{b}) + (\boldsymbol{\psi}_{b} - \boldsymbol{\psi}_{0}) \times \mathbf{n} \rangle_{\mathcal{E}_{h}} - s_{1}(e_{\lambda}, e_{\mathbf{q}}; \varphi, \boldsymbol{\psi})$$

$$- \langle \varepsilon(\tilde{\boldsymbol{\psi}} - \mathbb{Q}_{0}\tilde{\boldsymbol{\psi}}) \cdot \mathbf{n}, e_{s,0} - e_{s,b} \rangle_{\mathcal{E}_{h}}$$

$$= I_{1} + I_{2} + I_{3},$$

$$(5.14)$$

where we used the first error Eq. (5.1), $I_i(i = 1, ..., 3)$ are defined accordingly.

As to I_1 , using the same argument as what we did for (5.8), we get

$$|I_1| \le Ch^{k+\theta} \|\nabla^{k+\theta} \mathbf{u}\|_{I^q(\Omega)} \|(\varphi, \boldsymbol{\psi})\|. \tag{5.15}$$

As to I_2 , recalling the definition of s_1 and using the Cauchy-Schwarz inequality, we have

$$|I_{2}| \leq C \left(\sum_{T \in \mathcal{T}_{h}} h_{T}^{1-p} \int_{\partial T} |e_{\lambda,0} - e_{\lambda,b}|^{q(p-1)} ds \right)^{\frac{1}{q}} \left(\sum_{T \in \mathcal{T}_{h}} \int_{\partial T} h_{T}^{1-p} |\varphi_{0} - \varphi_{b}|^{p} ds \right)^{\frac{1}{p}}$$

$$+ C \left(\sum_{T \in \mathcal{T}_{h}} h_{T}^{1-p} \int_{\partial T} |e_{\mathbf{q},0} \times \mathbf{n} - e_{\mathbf{q},b} \times \mathbf{n}|^{q(p-1)} ds \right)^{\frac{1}{q}}$$

$$\cdot \left(\sum_{T \in \mathcal{T}_{h}} \int_{\partial T} h_{T}^{1-p} |\psi_{0} \times \mathbf{n} - \psi_{b} \times \mathbf{n}|^{p} ds \right)^{\frac{1}{p}}$$

$$\leq C \|(e_{\lambda}, e_{\mathbf{q}})\|^{\frac{p}{q}} \|(\varphi, \psi)\|.$$

$$(5.16)$$

Similarly, we use (5.4) and the approximation property of \mathbb{Q}_0 to get that

$$|I_3| \le Ch^{\alpha - \frac{1}{p}} \|\nabla^{\alpha} \tilde{\boldsymbol{\psi}}\|_{L^p(\Omega)} h^{\frac{q-1}{q}} \|\|\boldsymbol{e}_s\|\| = Ch^{\alpha} \|\nabla^{\alpha} \tilde{\boldsymbol{\psi}}\|_{L^p(\Omega)} \|\|\boldsymbol{e}_s\|.$$

$$(5.17)$$

It is easy to check

$$\|(\varphi, \psi)\| \le Ch^{\alpha - 1}(\|\tilde{\phi}\|_{\alpha, p} + \|\tilde{\psi}\|_{\alpha, p}). \tag{5.18}$$

Substituting (5.15)-(5.17) into (5.14), and using (5.5), (5.6), (5.11) and (5.18), this gives

$$|(\varepsilon(e_{\boldsymbol{u}}-\tilde{\boldsymbol{\eta}}),\boldsymbol{v}-\tilde{\boldsymbol{\eta}})| \leq Ch^{k+\theta}\|\nabla^{k+\theta}\boldsymbol{u}\|_{L^{q}(\Omega)}\|(\varphi,\boldsymbol{\psi})\| + Ch^{\alpha}\|\nabla^{\alpha}\tilde{\boldsymbol{\psi}}\|_{L^{p}(\Omega)}\|\|e_{s}\|$$

$$\leq Ch^{k+\theta+\alpha-1}\|\nabla^{k+\theta}\boldsymbol{u}\|_{L^{q}(\Omega)}\|\boldsymbol{v}-\tilde{\boldsymbol{\eta}}\|_{0,p}.$$

It follows that

$$\|\varepsilon^{\frac{1}{q}}(e_{\boldsymbol{u}}-\tilde{\boldsymbol{\eta}})\|_{L^{q}(\Omega)} \leq Ch^{k+\theta+\alpha-1}\|\nabla^{k+\theta}\boldsymbol{u}\|_{L^{q}(\Omega)},$$

which gives rise to the error estimate (5.12). This completes the proof of the theorem. \Box

6. Numerical experiments

In this section, we present some numerical examples to test the performance and accuracy of the PDWG method proposed in (3.4). In our numerical experiments, the computation domain is first partitioned into cubes, and then each cube is divided into 6 tetrahedra of equi-volume. We choose the discontinuous piecewise constant vector fields to approximate the exact solution \mathbf{u} . That is, the finite element spaces are given as follows:

$$\begin{aligned} & \boldsymbol{V}_{h} = \{ \boldsymbol{v} : \ \boldsymbol{v}|_{T} \in [P_{0}(T)]^{3}, \, \forall T \in \mathcal{T}_{h} \}, \\ & S_{h} = \{ \boldsymbol{s} : \ \boldsymbol{s}|_{T} = \{ \boldsymbol{s}_{0}, \boldsymbol{s}_{b} \} \in \{ P_{0}(T), \, \boldsymbol{\Pi}_{i=1}^{4} P_{0}(F_{i}) \}, \, \forall T \in \mathcal{T}_{h}, \, F_{i} \in \partial T \}, \\ & M_{h} = \{ \boldsymbol{\varphi} : \boldsymbol{\varphi}|_{T} = \{ \boldsymbol{\varphi}_{0}, \, \boldsymbol{\varphi}_{b} \} \in \{ P_{0}(T), \, \boldsymbol{\Pi}_{i=1}^{4} P_{0}(F_{i}) \}, \, \forall T \in \mathcal{T}_{h}, \, F_{i} \in \partial T \}, \\ & \boldsymbol{W}_{h} = \{ \boldsymbol{\psi} : \boldsymbol{\psi}|_{T} = \{ \boldsymbol{\psi}_{0}, \, \boldsymbol{\psi}_{h} \} \in \{ [P_{0}(T)]^{3}, \, T_{0}(\partial T) \}, \, \forall T \in \mathcal{T}_{h} \}, \end{aligned}$$

where $T_0(\partial T)$ is the tangent space of ∂T given by

$$T_0(\partial T) = \{ \boldsymbol{\psi} : \boldsymbol{\psi}_{i,i} \in [P_0(F_i)]^3 \times \mathbf{n}_{F_i}, F_i \in \partial T, i = 1, 2, 3, 4, j = 1, 2 \}.$$

Here \mathbf{n}_{F_i} denotes the outer unit normal vector to face F_i .

To solve the system of nonlinear Eq. (3.4), we adopt an iterative scheme similar to that for the L^1 minimization problem in [27]. Specifically, given an approximation $(\boldsymbol{u}_h^m, \lambda_h^m, s_h^m, \boldsymbol{q}_h^m) \in \boldsymbol{V}_h \times M_h \times S_h \times \boldsymbol{W}_h$ at step m, the scheme shall compute a new approximate solution $(\boldsymbol{u}_h^{m+1}, \lambda_h^{m+1}, \boldsymbol{s}_h^{m+1}, \boldsymbol{q}_h^{m+1}) \in \boldsymbol{V}_h \times M_h \times S_h \times \boldsymbol{W}_h$ such that

$$\begin{cases}
s_1(\lambda_h, \mathbf{q}_h; \varphi, \boldsymbol{\psi}) + B_h(\mathbf{u}_h, s_h; \varphi, \boldsymbol{\psi}) &= F(\varphi, \boldsymbol{\psi}), \quad \forall \varphi \in M_h, \ \boldsymbol{\psi} \in \mathbf{W}_h, \\
-s_2(s_h, r) + B_h(\boldsymbol{v}, r; \lambda_h, \mathbf{q}_h) &= 0, \quad \forall \boldsymbol{v} \in \mathbf{V}_h, \ r \in S_h.
\end{cases}$$
(6.1)

where

$$s_{1}(\lambda_{h}, \boldsymbol{q}_{h}; \varphi, \boldsymbol{\psi}) = \rho_{1} \sum_{T \in \mathcal{T}_{h}} h_{T}^{1-p} \int_{\partial T} (|\lambda_{0}^{m} - \lambda_{b}^{m}| + \epsilon_{0})^{p-2} (\lambda_{0}^{m+1} - \lambda_{b}^{m+1}) (\varphi_{0} - \varphi_{b}) ds$$

$$+ \rho_{2} \sum_{T \in \mathcal{T}_{h}} h_{T}^{1-p} \int_{\partial T} (|\boldsymbol{q}_{0}^{m} \times \boldsymbol{n} - \boldsymbol{q}_{b}^{m} \times \boldsymbol{n}| + \epsilon_{0})^{p-2} (\boldsymbol{q}_{0}^{m+1} \times \boldsymbol{n} - \boldsymbol{q}_{b}^{m+1} \times \boldsymbol{n}) (\boldsymbol{\psi}_{0} \times \boldsymbol{n} - \boldsymbol{\psi}_{b} \times \boldsymbol{n}) ds,$$

Numeric	al error and rat	e of convergence for	the L^p -PDWG me	ethod for Example 6.1			
p	1/h	$\ arepsilon^{rac{1}{q}}\mathbf{e}_h\ _{L^q}$	rate	$ \! \! (e_{\lambda},e_{\boldsymbol{q}}) \! \! $	rate	$ s_h $	rate
	2	1.52e-01	-	3.27e-02	_	1.52e-03	_
2	4	7.67e-02	0.99	1.82e-02	0.84	3.05e-04	2.32
	8	3.82e-02	1.00	9.37e-03	0.96	5.10e-05	2.58
	16	1.91e-02	1.00	4.72e-03	0.99	9.29e-06	2.46
	2	1.73e-01	_	2.84e-01	-	2.47e-03	_
3	4	8.65e-02	1.00	1.99e-01	0.52	3.20e-04	2.95
	8	4.27e-02	1.02	1.30e-01	0.61	3.78e-05	3.08
	16	2.17e-02	0.98	8.01e-02	0.70	5.03e-06	2.91
	2	1.97e-01	_	4.26e-01	-	2.30e-03	_
4	4	1.02e-01	0.95	3.05e-01	0.48	2.31e-04	3.31
	8	5.51e-02	0.88	2.07e-01	0.56	1.80e-05	3.68
	16	2.92e-02	0.92	1.41e-01	0.55	1.59e-06	3.50
	2	2.13e-01	-	4.16e-01	-	5.79e-04	-
5	4	1.21e-01	0.82	3.02e-01	0.46	4.29e-05	3.76
	8	6.38e-02	0.92	2.25e-01	0.43	2.89e-06	3.89
	16	3.20e_02	1.00	1.70e_01	0.40	3 11e-07	3 22

Table 1Numerical error and rate of convergence for the IP-PDWC method for Example 6.1

$$s_2(s_h; r) = \rho_3 \sum_{T \in \mathcal{T}_h} h_T^{1-q} \int_{\partial T} (|s_0^m - s_b^m| + \epsilon_0)^{q-2} (s_0^{m+1} - s_b^{m+1}) (r_0 - r_b) ds.$$

Here ϵ_0 is a small, but positive constant, and ρ_i , $i \leq 3$ are some positive stabilization parameters.

We would like to point out that although ρ_i , $i \le 3$ in the algorithm (3.4) could be arbitrary, the iterative scheme (6.1) is not convergent for any positive ρ_i , $i \le 3$. Our numerical experiments indicate that ρ_i , i = 1, 2 should be taken large enough to ensure the convergence of the iterative scheme.

In our experiments, we test various problems in which the exact solution \mathbf{u} has different regularities and the computational domain includes convex, non-convex polyhedral regions and cavities. We shall evaluate the errors for both \mathbf{u}_h and the auxiliary variables λ_h , s_h , \mathbf{q}_h , including the L^q error for $\mathbf{e}_h := \mathbf{u} - \mathbf{u}_h$ and $\eta_h := \mathcal{Q}_h \mathbf{u} - \mathbf{u}_h$, and the errors $\|(e_\lambda, e_q)\|$ and $\|s_h\|$ defined in (4.1) and (4.2). We test different values of p > 1 with p = 2, 3, 4, 5. The right-hand side function, the boundary condition are calculated from the exact solution. The coefficient ϵ_0 in (6.1) is taken as $\epsilon = 10^{-6/(p-1)}$, $\rho_3 = 1$, and ρ_i , i = 1, 2 are carefully taken according to different problems. We stop our iterative procedure when the maximum error between the mth step and the (m+1)-th step reaches the accuracy 10^{-5} .

Example 6.1. In this test, we consider the model problem (1.1) in the domain $\Omega = (0, 1)^3$ with $\varepsilon = \text{diag}(3, 2, 1)$. The right-hand side function and the boundary condition are chosen such that the exact solution to this problem is

$$\mathbf{u}(x, y, z) = \begin{pmatrix} \sin(\pi x)\cos(\pi y) \\ -\sin(\pi y)\cos(\pi x) \\ 0 \end{pmatrix} + \begin{pmatrix} x \\ y \\ z \end{pmatrix}.$$

It is easy to see that $\mathbf{u} \in [H^1(\Omega)]^3$.

The problem is solved by (6.1) with the coefficients $\rho_1 = \rho_2 = 1$ for p = 2 and $\rho_1 = \rho_2 = 9 \times 10^{p-1}$ for $p \ge 2$. Table 1 illustrates the approximation error and the rate of convergence for the primal variable \mathbf{u}_h and the auxiliary variables λ_h , s_h , \mathbf{q}_h with $p = 2, \ldots, 5$. We observe a convergence rate of $\mathcal{O}(h)$ for the error $\|\varepsilon^{\frac{1}{q}}\mathbf{e}_h\|_{L^q}$. For the dual variables λ_h , \mathbf{q}_h , the table suggests a p-dependence rate of the convergence, i.e., $\mathcal{O}(h)$ for p = 2, $\mathcal{O}(h^{0.6})$ for p = 3, $\mathcal{O}(h^{0.55})$ for p = 4 and $\mathcal{O}(h^{0.4})$ for p = 5. Note that the convergence rate of $\|(e_\lambda, e_q)\|$ is slightly higher than the theoretical result $\mathcal{O}(h^{\frac{q}{p}})$ in (5.5). As for the dual variable s_h , we observe a better convergence rate than the theoretical finding $\mathcal{O}(h)$ given in (5.6), which indicates a superconvergence result.

Example 6.2. The domain in this test case is the *L*-shape domain, which is given by $\Omega = (0, 1)^3 \setminus \Omega_1$ with $\Omega_1 = [0, 1] \times [-1, 0] \times [0, 1]$. We take the coefficient $\epsilon = \text{diag}(1, 1, 1)$ and the singular solution in $[H^{2/3-\delta}(\Omega)]^3$:

$$\mathbf{u} = \nabla \times (0, 0, r^{2/3} \sin(\frac{2}{3}\theta)).$$

Here $r = \sqrt{x^2 + y^2}$ and $\theta = \arctan(y/x) + c$ are the cylindrical coordinates. We take c such that $\mathbf{u} \in H(div) \cap H(curl)$.

We take the iterative scheme (6.1) to solve this paper with the same coefficient choice of ρ_1 , ρ_2 as Example 6.1. Numerical error and rate of convergence for the L^p -PDWG method are listed in Table 2, from which we observe an optimal

Table 2 Numerical error and rate of convergence for the L^p -PDWG method for Example 6.2.

		•					
p	1/h	$\ arepsilon^{rac{1}{q}}\mathbf{e}_h\ _{L^q}$	rate	$ (e_{\lambda},e_{m{q}}) $	rate	$ s_h $	rate
	2	1.28e-01	-	3.70e-02	_	1.02e-03	_
2	4	8.25e-02	0.64	2.42e-02	0.61	3.18e-04	1.69
	8	5.28e-02	0.64	1.55e-02	0.64	9.66e-05	1.72
	16	3.35e-02	0.65	9.92e-03	0.65	2.96e-05	1.71
	2	1.69e-01	_	1.96e-01	-	1.37e-04	_
3	4	9.82e-02	0.78	1.44e-01	0.44	3.10e-05	2.15
	8	5.77e-02	0.77	1.01e-01	0.52	6.29e-06	2.30
	16	3.39e-02	0.77	6.66e-02	0.59	1.05e-06	2.58
	2	2.00e-01	_	3.54e-01	-	2.19e-04	_
4	4	1.18e-01	0.76	2.63e-01	0.43	2.77e-05	2.98
	8	6.81e-02	0.79	1.67e-01	0.65	1.79e-06	3.95
	16	3.65e-02	0.90	9.79e - 02	0.77	6.91e-08	4.70
	2	2.18e-01	_	3.75e-01	-	5.47e-05	-
5	4	1.34e-01	0.70	2.30e-01	0.71	1.16e-06	5.56
	8	7.12e-02	0.91	1.29e-01	0.83	1.15e-08	6.66
	16	3.61e-02	0.98	7.15e-02	0.85	1.00e-10	6.84

Table 3 Numerical error and rate of convergence for the L^p -PDWG method for Example 6.3.

p	1/h	$\ \varepsilon^{\frac{1}{q}}\mathbf{e}_h\ _{L^q}$	rate	$\ (e_{\lambda}, e_{q})\ $	rate	S _h	rate
	2	1.49e-00	_	3.48e-00	-	5.16e-01	-
2	4	1.02e-00	0.55	2.60e-00	0.42	2.66e-01	0.96
	8	6.84e-01	0.57	1.86e-00	0.48	1.01e-01	1.39
	16	4.69e-01	0.55	1.30e-00	0.51	3.49e - 02	1.54
	2	1.79e-00	-	6.45e-01	-	3.75e-04	-
3	4	1.21e-00	0.57	5.14e-01	0.33	1.24e-04	1.60
	8	8.12e-01	0.57	4.02e-01	0.35	4.14e-05	1.59
	16	5.70e-01	0.51	3.12e-01	0.37	1.28e-05	1.69
	2	2.07e-00	_	1.22e-00	_	5.38e-03	-
4	4	1.41e-00	0.55	1.03e-00	0.25	1.50e-03	1.84
	8	9.77e-01	0.53	8.60e-01	0.26	4.30e-04	1.80
	16	6.78e-01	0.53	7.17e-01	0.26	1.24e-04	1.80
	2	2.18e-00	_	9.54e-01	_	9.98e-04	-
5	4	1.57e-00	0.47	8.30e-01	0.20	2.77e-04	1.82
	8	1.06e-00	0.56	7.19e-01	0.21	7.67e-05	1.85
	16	7.33e-01	0.53	6.22e-01	0.21	2.12e-05	1.86

convergence rate $\mathcal{O}(h^{\frac{2}{3}})$ for the errors $\|\varepsilon^{\frac{1}{q}}\mathbf{e}_h\|_{L^q}$ and $\|(e_\lambda,e_q)\|$ for p=2. While, as p increases, the convergence rate for \mathbf{u}_h is improved from $\mathcal{O}(h^{\frac{2}{3}})$ to $\mathcal{O}(h)$ (for p=5). Like in Example 6.1, the numerical convergence for the dual variables is faster than the theory predicted in Theorem 5.1.

Example 6.3. In this example, we test a singular solution in the following vector potential form on a toroidal domain with 2 holes: $\Omega = [(-1, \frac{3}{2})]^2 \setminus \{\Omega_1 \cup \Omega_2\}$ with $\Omega_1 = [-\frac{1}{2}, 0]^2 \times [0, \frac{1}{2}]$ and $\Omega_2 = [\frac{1}{2}, 1] \times [-\frac{1}{2}, 0] \times [0, \frac{1}{2}]$. We take $\epsilon = \text{diag}(1, 1, 1)$ and

$$\mathbf{u} = \nabla \times (0, 0, r_1^{\gamma_1} \sin(2\theta_1) + r_2^{\gamma_2} \sin(2\theta_2)),$$

where (r_i, θ_i) , i = 1, 2 are the cylindrical coordinates centered at a nonconvex corner of the *i*th hole. That is,

$$r_1 = \sqrt{x^2 + y^2}$$
, $\theta_1 = \arctan(y/x) + c_1$, $r_2 = \sqrt{(x-1)^2 + y^2}$, $\theta_2 = \arctan(y/x) + c_2$.

In our numerical experiments, we choose $\gamma_1 = 1/2$, $\gamma_2 = 2/3$ such that the vector field is singular near the nonconvex corners of both holes. Note that $\mathbf{u} \in H^{\frac{1}{2}-\delta}$ in a neighborhood of the edge $\{x = 0, y = 0\}$, and $\mathbf{u} \in H^{\frac{2}{3}-\delta}$ in a neighborhood of the edge $\{x = 1, y = 0\}$.

From Table 3, we observe a convergence rate of $\mathcal{O}(h^{\frac{1}{2}})$ for the error $\|\varepsilon^{\frac{1}{q}}\mathbf{e}_h\|_{L^q}$, and $\mathcal{O}(h^{\frac{1}{p}})$ for the error $\|(e_\lambda, e_q)\|$ with $p=2,\ldots,5$. Again, it seems that the convergence rate for $\|s_h\|$ is better than the theory predicted in Theorem 5.1.

Table 4 Numerical error and rate of convergence for the L^p -PDWG method with $\gamma = 5/4$ for Example 6.4.

		0		• ,			
p	1/h	$\ \varepsilon^{\frac{1}{q}}\mathbf{e}_h\ _{L^q}$	rate	$\ (e_{\lambda}, e_{\boldsymbol{q}})\ $	rate	s _h	rate
	2	3.96e-01	_	9.07e-01	_	6.51e-02	_
2	4	2.07e-01	0.93	5.01e-01	0.86	3.23e-02	1.01
	8	1.06e-01	0.97	2.67e-01	0.91	9.48e-03	1.77
	16	5.38e-02	0.98	1.39e-01	0.95	2.17e-03	2.12
	2	4.61e-01	_	4.14e-01	-	4.17e-04	_
3	4	2.39e-01	0.95	2.88e-01	0.53	1.05e-04	1.99
	8	1.27e-01	0.91	1.94e-01	0.57	2.20e-05	2.25
	16	6.65e-02	0.94	1.25e-01	0.63	4.23e-06	2.38
	2	4.92e-01	-	5.92e-01	-	5.23e-04	_
4	4	2.67e-01	0.88	4.29e-01	0.46	1.05e-04	2.31
	8	1.41e-01	0.92	3.04e-01	0.50	1.78e-05	2.57
	16	7.23e-02	0.97	2.16e-01	0.50	2.74e - 06	2.70
	2	5.33e-01	_	8.43e-01	_	3.56e-03	_
5	4	2.93e-01	0.86	6.50e-01	0.38	6.15e-04	2.53
	8	1.50e-01	0.97	4.98e-01	0.39	1.04e-04	2.56
	16	7.55e-02	0.99	3.80e-01	0.39	1.54e-05	2.75

Table 5 Numerical error and rate of convergence for the L^p -PDWG method with $\gamma = 1$ for Example 6.4.

p	1/h	$\ arepsilon^{rac{1}{q}}\mathbf{e}_{h}\ _{L^{q}}$	rate	$ \! \! (e_{\lambda},e_{\boldsymbol{q}}) \! \! $	rate	$ s_h $	rate
	2	5.33e-01	_	1.22e-00	_	1.14e-01	_
2	4	3.01e-01	0.83	7.27e-01	0.74	5.65e-02	1.01
	8	1.63e-01	0.88	4.15e-01	0.81	1.79e-02	1.66
	16	8.86e-02	0.88	2.30e-01	0.85	4.62e-03	1.96
	2	6.02e-01	_	5.84e-01	_	1.22e-03	_
3	4	3.29e-01	0.87	3.98e-01	0.55	2.55e-04	2.26
	8	1.87e-01	0.82	2.78e-01	0.52	5.63e-05	2.18
	16	1.03e-01	0.86	1.88e-01	0.56	1.22e-05	2.21
	2	6.50e-01	_	7.57e-01	-	1.26e-03	_
4	4	3.80e-01	0.77	5.68e-01	0.41	2.52e-04	2.32
	8	2.14e-01	0.83	4.19e-01	0.44	4.91e-05	2.36
	16	1.13e-01	0.93	3.07e-01	0.45	9.16e-06	2.42
	2	6.88e-01	_	8.31e-01	_	1.60e-03	-
5	4	4.14e-01	0.73	6.57e-01	0.34	3.09e - 04	2.38
	8	2.26e-01	0.87	5.16e-01	0.35	5.79e-05	2.41
	16	1.19e-01	0.93	4.04e-01	0.35	1.01e-05	2.52

Example 6.4. In this test, we consider a singular solution in the following vector potential form on a toroidal domain with 1 holes: $\Omega = [(-1, \frac{1}{2})]^2 \times [0, \frac{1}{2}] \setminus \Omega_1$ with $\Omega_1 = [-\frac{1}{2}, 0] \times [0, \frac{1}{2}]^2$. We take $\epsilon = \text{diag}(1, 1, 1)$ and

$$\mathbf{u} = \nabla \times (0, 0, r^{\gamma} \sin(2\theta)).$$

We consider three cases: $\gamma = 5/4$, 1, 2/3, where the regularity of the exact solution ranges from smooth to singular.

The coefficients ρ_1 , ρ_2 in (6.1) are chosen as following: $\rho_1 = \rho_2 = 1$ for p = 2, $\rho_1 = \rho_2 = 3 \times 10^3$ for p = 3 and $\rho_1 = \rho_2 = 3 \times 10^4$ for $p \ge 4$. Numerical error and rate of convergence for the L^p -PDWG method with different γ are listed in Tables 4–6. We observe the following result:

- Regular solution, i.e., γ = 5/4, ||ε^{1/q} e_h||_{L^q} has optimal convergence rate O(h) for all p ≥ 2, |||(e_λ, e_q)|| has optimal convergence rate O(h) for p = 2, and p-dependency rate when p ≥ 3, which is slightly better than the theoretical rate O(h^{1/p}). As for s_h, a superconvergent order still observed in this cases.
 Singular case γ = 1, where u ∈ H^{1-δ} and u ∉ H(curl). An asymptotical rate of O(h^{0.9}) is observed for the error
- Singular case $\gamma = 1$, where $\mathbf{u} \in H^{1-\delta}$ and $\mathbf{u} \notin H(curl)$. An asymptotical rate of $\mathcal{O}(h^{0.9})$ is observed for the error $\|\varepsilon^{\frac{1}{q}}\mathbf{e}_h\|_{L^q}$ with all $p \geq 2$. The convergence behavior for the auxiliary variable are the same as that for the regular case $\gamma = \frac{5}{2}$.
- Singular case $\gamma = 2/3$, where $\mathbf{u} \in H^{\frac{2}{3}-\delta}$ and $\mathbf{u} \notin H(curl)$. $\|\varepsilon^{\frac{1}{q}}\mathbf{e}_h\|_{L^q}$ has an optimal convergence rate $\mathcal{O}(h^{\frac{2}{3}})$ for all $p \geq 2$, and $\|(\mathbf{e}_{\lambda}, \mathbf{e}_{\mathbf{q}})\|$ shows a rate of $\mathcal{O}(h^{0.6})$ for p = 2 and $\mathcal{O}(h^{\frac{q}{p}})$ for all $p \geq 3$.

Example 6.5. In this test, we reveal some computational results for a test problem where the existence of a harmonic vector field has effect on convergence rate. We consider the problem on a toroidal domain with 2 holes, which is the

Table 6
Numerical error and rate of convergence for the I^p -PDWG method with $\nu = 2/3$ for Example 6.4.

p	1/h	$\ \varepsilon^{\frac{1}{q}}\mathbf{e}_h\ _{L^q}$	rate	$\ (e_{\lambda},e_{q})\ $	rate	s _h	rate
	2	8.87e-01	_	2.09e-00	_	2.77e-01	-
2	4	5.77e-01	0.62	1.45e-00	0.52	1.38e-01	1.01
	8	3.62e-01	0.68	9.67e-01	0.59	4.92e-02	1.49
	16	2.29e-01	0.66	6.26e-01	0.63	1.55e-02	1.67
	2	1.02e-00	_	8.04e-01	-	2.07e-03	_
3	4	6.16e-01	0.73	5.77e-01	0.48	4.91e-04	2.08
	8	3.94e - 01	0.64	4.37e-01	0.40	1.39e-04	1.82
	16	2.47e-01	0.67	3.28e-01	0.42	4.21e-05	1.73
	2	1.07e-00	_	1.06e-00	_	4.46e-03	_
4	4	7.10e-01	0.59	8.64e-01	0.30	1.13e-03	1.98
	8	4.63e-01	0.62	6.93e-01	0.32	2.86e-04	1.98
	16	2.90e-01	0.67	5.53e-01	0.32	7.19e-05	1.99
	2	1.11e-00	_	1.09e-00	_	5.79e-03	_
5	4	7.73e-01	0.52	9.19e-01	0.25	1.41e-03	2.04
	8	4.94e - 01	0.65	7.71e-01	0.25	3.44e - 04	2.03
	16	3.09e-01	0.68	6.45e-01	0.26	8.25e-05	2.06

Table 7 Numerical error and rate of convergence for the L^p -PDWG method for Example 6.5.

p	1/h	$\ arepsilon^{rac{1}{q}}\mathbf{e}_h\ _{L^q}$	rate	$\ arepsilon^{rac{1}{q}} oldsymbol{\eta}_h\ _{L^q}$	rate	$ \! \! (e_{\lambda},e_{\pmb{q}}) \! \! $	rate	$\ s_h\ $	rate	It.
	2	2.60e-01	-	1.90e-01	_	3.79e-01	-	5.83e-02	-	1
2	4	2.03e-01	0.36	1.69e-01	0.17	2.55e-01	0.57	2.93e-02	0.99	1
	8	1.70e-01	0.26	1.54e-01	0.13	1.67e-01	0.61	1.03e-02	1.51	1
	16	1.53e-01	0.15	1.46e-01	0.08	1.07e-01	0.64	3.26e-03	1.66	1
-	2	2.78e-01	-	2.16e-01	-	1.35e-01	-	1.52e-05	-	14
3	4	2.28e-01	0.29	2.02e-01	0.09	9.93e-02	0.44	4.98e-06	1.60	15
	8	1.98e-01	0.20	1.88e-01	0.11	7.11e-02	0.48	1.20e-06	2.06	18
	16	1.80e-01	0.14	1.76e-01	0.09	5.06e-02	0.49	2.88e-07	2.06	19
-	2	3.12e-01	-	2.55e-01	-	3.98e-01	-	1.60e-04	0	18
4	4	2.62e-01	0.25	2.40e-01	0.09	3.12e-01	0.35	4.54e-05	1.82	28
	8	2.25e-01	0.22	2.15e-01	0.15	2.45e-01	0.35	1.08e-05	2.07	28
	16	1.99e-01	0.18	1.95e-01	0.14	1.93e-01	0.34	2.60e-06	2.05	26
	2	3.42e-01	-	2.87e-01	-	6.12e-01	-	8.62e-04	-	29
5	4	2.84e-01	0.27	2.63e-01	0.13	5.05e-01	0.28	2.32e-04	1.89	23
	8	2.37e-01	0.26	2.28e-01	0.20	4.19e-01	0.27	5.59e-05	2.06	24
	16	2.08e-01	0.19	2.04e-01	0.16	3.48e-01	0.27	1.31e-05	2.09	30

same as that in Example 6.3. We take $\epsilon = \text{diag}(1, 1, 1)$ and

$$\mathbf{u} = \nabla \times (0, 0, r_1^{\gamma_1} \sin(\theta_1) + r_2^{\gamma_2} \sin(\theta_2)) + \beta \begin{pmatrix} e^y \sin(z) \\ e^x \sin(z) \\ z \end{pmatrix}$$

with
$$(\gamma_1, \gamma_2, \beta) = (\frac{4}{5}, \frac{2}{3}, \frac{1}{40})$$
.

The coefficients ρ_1 , ρ_2 in (6.1) are chosen as following: $\rho_1 = \rho_2 = 1$ for p = 2, $\rho_1 = \rho_2 = 5 \times 10^4$ for $p \ge 3$. The plot of the vector field η_h is provided in Fig. 1, and the errors and rates of convergence of the L^p -PDWG method for the primal variable and the dual variables are given in Table 7. As indicated by Theorem 5.2, the numerical solution \mathbf{u}_h approximates the exact solution \mathbf{u}_h up to a harmonic field. As we may observe from Fig. 1, the vector field η_h is an approximate harmonic field with normal boundary condition. Furthermore, due to the presence of the harmonic field vector, the error η_h or \mathbf{e}_h may not exhibit a convergence. Our numerical result in Table 7 verifies this point. We do not observe any convergence for the vector field \mathbf{u}_h . It is noteworthy that although the vector field \mathbf{u}_h is not convergent to \mathbf{u}_h while our iterative algorithm is still convergent. We list in Table 7 that the iterative number used in the iterative procedure. As for the dual variable λ_h , \mathbf{q}_h , we observe a rate of $\mathcal{O}(h^{\frac{q}{p}})$ for $p \ge 3$. The numerical performance is in consistency with our theory as established in Theorem 5.1 for the convergence of e_λ , $e_{\mathbf{q}}$. The convergence rate for s_h is still better than the one given in (5.6).

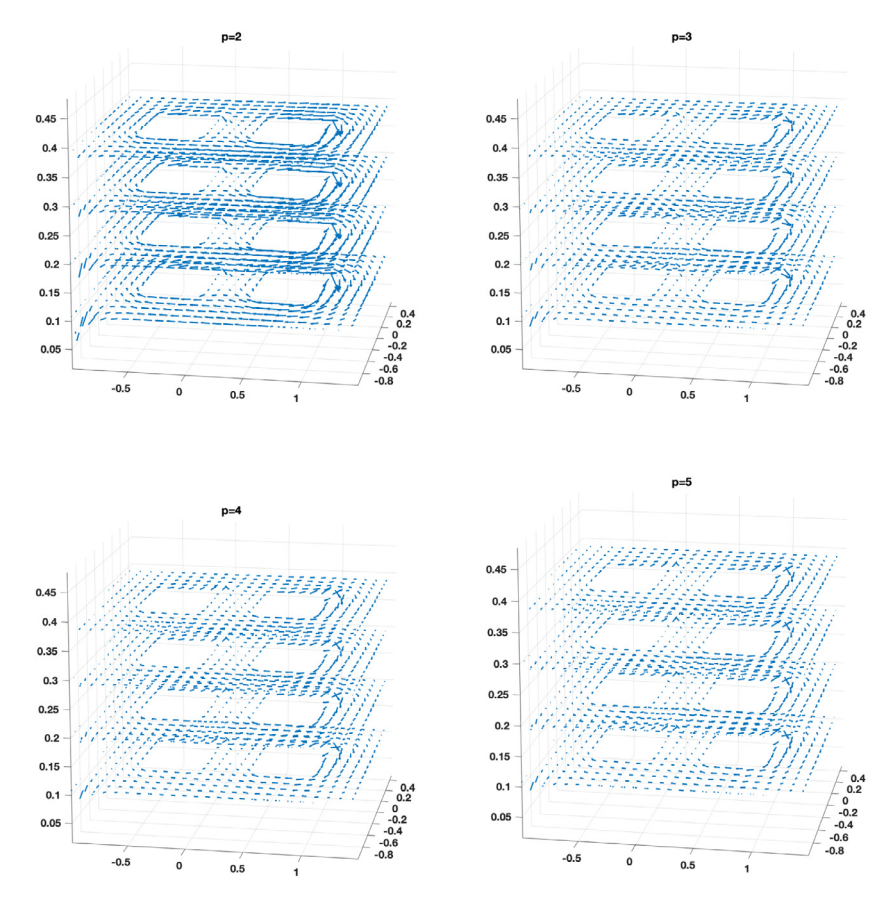


Fig. 1. Plot of the vector fields η_h calculated by the L^p -PDWG method of Example 6.5 with different values of p.

Table 8 Numerical error and rate of convergence for the L^p -PDWG method for Example 6.6.

p	1/h	$\ arepsilon^{rac{1}{q}}\mathbf{e}_h\ _{L^q}$	rate	$\ arepsilon^{rac{1}{q}} oldsymbol{\eta}_h\ _{L^q}$	rate	$ \! \! (e_{\lambda},e_{\boldsymbol{q}}) \! \! $	rate	$ s_h $	rate	It.
	2	2.18e-01	_	1.61e-01	_	2.98e-01	-	5.18e-02	-	1
2	4	1.75e-01	0.32	1.45e-01	0.15	2.16e-01	0.46	2.67e-02	0.95	1
	8	1.47e-01	0.25	1.33e-01	0.13	1.47e-01	0.56	9.49e - 03	1.50	1
	16	1.33e-01	0.15	1.26e-01	0.07	9.61e-02	0.61	3.04e-03	1.64	1
	2	2.14e-01	-	1.67e-01	-	1.14e-01	-	1.19e-05	-	14
3	4	1.81e-01	0.24	1.60e-01	0.06	8.85e-02	0.37	4.29e-06	1.48	16
	8	1.58e-01	0.19	1.49e-01	0.10	6.51e-02	0.44	1.05e-06	2.03	18
	16	1.45e-01	0.13	1.41e-01	0.08	4.72e-02	0.47	2.58e-07	2.03	19
	2	2.28e-01	-	1.85e-01	-	3.56e-01	-	1.27e-04	-	18
4	4	1.99e-01	0.20	1.81e-01	0.03	2.89e-01	0.30	3.89e-05	1.7	30
	8	1.73e-01	0.20	1.66e-01	0.13	2.30e-01	0.33	9.44e - 06	2.04	28
	16	1.54e-01	0.17	1.51e-01	0.13	1.84e-01	0.33	2.33e-06	2.02	26
	2	2.42e-01	-	2.01e-01	_	5.63e-01	_	7.06e-04	_	18
5	4	2.11e-01	0.20	1.94e-01	0.05	4.75e-01	0.24	1.99e-04	1.83	24
	8	1.79e-01	0.23	1.72e-01	0.17	3.99e-01	0.25	4.86e-05	2.03	24
	16	1.58e-01	0.18	1.55e-01	0.15	3.35e-01	0.26	1.16e-05	2.06	31

Example 6.6. In this test, we consider the problem on a toroidal domain with 1 holes, which is the same as that in Example 6.4. We take $\epsilon = \text{diag}(1, 1, 1)$ and

$$\mathbf{u} = \nabla \times (0, 0, r^{\gamma} \sin(\theta)) + \beta \begin{pmatrix} \sin(\pi x) \cos(\pi y) \sin(\pi z) \\ \cos(\pi x) \sin(\pi y) \sin(\pi z) \\ 0 \end{pmatrix}$$

with
$$(\gamma, \beta) = (\frac{2}{3}, \frac{1}{8})$$
.

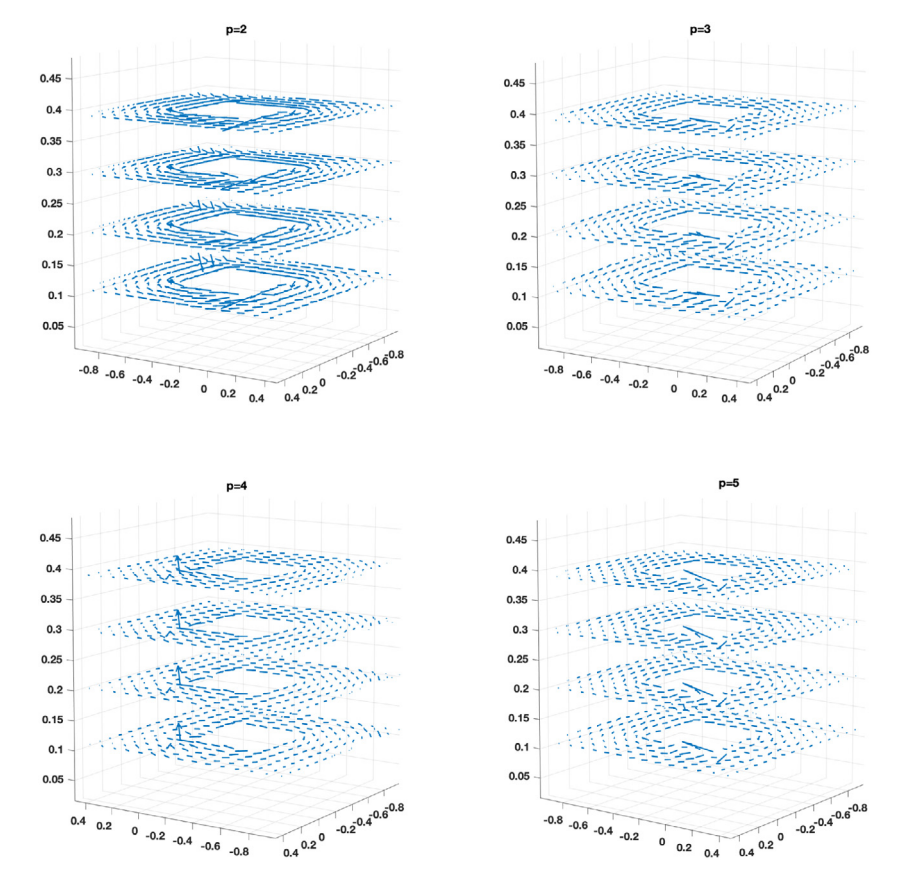


Fig. 2. Plot of the vector fields η_b calculated by the L^p -PDWG method of Example 6.6 with different values of p.

We take the iterative parameters as those in Example 6.5, and plot the vector field η_h in Fig. 2, and present in Table 8 the errors and rates of convergence for the primal variable and the dual variables approximation. Just the same as that in Example 6.5, the numerical results do not demonstrate any convergence for the vector field \mathbf{u} , while show a rate of $\mathcal{O}(h^{\frac{q}{p}})$ for $\|(e_\lambda, e_q)\|$ and a superconvergence rate $\mathcal{O}(h^2)$ for $\|s_h\|$ when $p \geq 3$. Again we observe that the iterative scheme is still convergent and the vector field η_h is an approximate harmonic field with normal boundary condition.

Data availability

Data will be made available on request.

References

- [1] J. Li, Y. Huang, Time-Domain Finite Element Methods for Maxwell's Equations in Metamaterials, Springer, 2013.
- [2] R. Nicolaides, X. Wu, Covolume solutions of three-dimensional div-curl equations, SIAM J. Numer. Anal. 34 (1997) 2195-2203.
- [3] P.B. Bochev, K. Peterson, C.M. Siefert, Analysis and computation of compatible least-squares methods for div-curl equations, SIAM J. Numer. Anal. 49 (2011) 159–181.
- [4] R. Bensow, M.G. Larson, Discontinuous least-squares finite element method for the div-curl problem, Numer. Math. 101 (2005) 601-617.
- [5] A. Bossavit, Computational Electromagnetism, Academic Press, San Diego, 1998.
- [6] R.A. Nicolaides, Direct discretization of planar div-curl problems, SIAM J. Numer. Anal. 29 (1992) 32-56.
- [7] S. Delcourte, K. Domelevo, P. Omnes, A discrete duality finite volume approach to Hodge decomposition and div-curl problems on almost arbitrary two-dimensional meshes, SIAM J. Numer. Anal. 45 (2007) 1142–1174.
- 8] D.M. Copeland, J. Gopalakrishnan, J.E. Pasciak, A mixed method for axisymmetric div-curl systems, Math. Comp. 77 (2008) 1941-1965.
- [9] R. Brezzi, A. Buffa, Innovative mimetic discretizations for electromagnetic problems, J. Comput. Appl. Math. 234 (2010) 1980-1987.
- [10] K. Lipnikov, G. Manzini, F. Brezzi, A. Buffa, The mimetic finite difference method for the 3D magnetostatic field problems on polyhedral meshes, J. Comput. Phys. 230 (2011) 305–328.
- [11] C. Wang, J. Wang, Discretization of div-curl systems by weak Galerkin finite element methods on polyhedral partitions, J. Sci. Comput. 68 (2016) 1144-1171.
- [12] J. Li, X. Ye, S. Zhang, A weak Galerkin least-squares finite element method for div-curl systems, J. Comput. Phys. 363 (2018) 79–86.
- [13] Y. Liu, J. Wang, A primal-dual weak Galerkin method for div-curl systems with low-regularity solutions, arXiv preprint arXiv:2003.11795v2.
- [14] S. Cao, C. Wang, J. Wang, A new numerical method for div-curl Systems with Low Regularity Assumptions, arXiv preprint arXiv:2101.03466.

- [15] W. Cao, C. Wang, Applied Numerical Mathematics 162 (2021) 171-191,
- [16] D. Li, C. Wang, J. Wang, Primal-dual weak galerkin finite element methods for linear convection equations in non-divergence form, Journal of Computational and Applied Mathematics 412 (2022) 114313.
- [17] C. Wang, A new primal-dual weak Galerkin finite element method for ill-posed elliptic Cauchy problems, J. Comput. Appl. Math. (2019)
- [18] C. Wang, J. Wang, A primal-dual finite element method for first-order transport problems, J. Comput. Phys. 417 (2020) 109571.
- [19] C. Wang, J. Wang, A primal-dual weak galerkin finite element method for second order elliptic equations in non-divergence form, Math. Comp. 87 (2018) 515-545.
- [20] C. Wang, J. Wang, A primal-dual weak galerkin finite element method for Fokker-Planck type equations, SIAM J. Numer. Anal 58 (5) (2020) 2632-2661.
- [21] C. Wang, J. Wang, Primal-dual weak galerkin finite element methods for elliptic cauchy problems, Comput. Math. Appl. 79 (3) (2020) 746-763.
- [22] C. Wang, L. Zikatanov, Low regularity primal-dual weak galerkin finite element methods for convection-diffusion equations, Journal of Computational and Applied Mathematics 394 (2021) 113543.
- [23] W. Cao, C. Wang, J. Wang, An L^p-primal-dual weak galerkin method for convection-diffusion equations, Journal of Computational and Applied Mathematics 419 (2023) 114698.
- [24] P.G. Ciarlet, The Finite Element Method for Elliptic Problems, North-Holland, 1978.
- [25] V. Girault, P.-A. Raviart, Finite Element Methods for Navier-Stokes Equations: Theory and Algorithms, Springer-Verlag Berlin Heidelberg, 1986.
- [26] J. Wang, X. Ye, A weak galerkin mixed finite element method for second-order elliptic problems, Math. Comp. 83 (2014) 2101-2126.
- [27] C. Vogel, M. Oman, Iterative methods for total variation denoising, SIAM J. Sci. Comput. 17 (1996) 227-238.